Biochemical Characterization of Decellularized Human Lung ECM with Focus on Sex-Based Differences

Lea Miller, Caymen Novak

Department of Mechanical Engineering, Bioengineering Program, University of Michigan Dearborn, 4901 Evergreen Rd, Dearborn, MI 48128



A dissertation (thesis) submitted in partial fulfillment
of the requirements for the degree of
MS Bioengineering
in The University of Michigan-Dearborn
2026

Masters Thesis Committee:
Dr Caymen Novak – Assistant Professor, Chair
Dr Alan Argento – Professor, Director of Bioengineering Program
Dr Aditya Raghunandan – Assistant Professor

Abstract

The lung is a structurally complex organ whose native extracellular matrix (ECM) is difficult to replicate in vitro. Because the ECM provides critical biochemical and mechanical cues that regulate cell behavior, decellularized human lung tissue offers a tissue-specific material for studying how retained matrix composition is shaped by processing conditions and biological sex. This study compared two human lung decellularization methods containing either 0.1% or 0.5% sodium dodecyl sulfate (SDS), evaluated decellularization efficacy, and characterized sex-based differences in retained ECM composition. Healthy male and female human lung tissues were analyzed, with preliminary idiopathic pulmonary fibrosis (IPF) samples included for exploratory comparison. Decellularization efficacy was assessed using DNA quantification, DAPI staining, and agarose gel electrophoresis. Retained total protein, insoluble collagen, soluble collagen, elastin, and sulfated glycosaminoglycans (sGAG) were quantified under wet- and dry-weight normalization, and cytocompatibility was evaluated using NIH 3T3 fibroblasts in conditioned-media and direct-contact culture. Both protocols effectively removed cellular material, but matrix preservation was strongly method dependent. Overall, the 0.1% SDS condition retained more total protein and several key ECM components than the 0.5% SDS condition. Sex-based differences were also observed, and preliminary IPF data suggested that both disease state and sex may influence retained matrix composition. Together, these findings show that decellularization method and sex shape the biochemical identity of human lung dECM and support future sex-aware lung ECM platforms for disease modeling and mechanobiology studies.

Keywords: Lung decellularization, ECM, composition, biomaterial, sex based differences, mechanobiology, idiopathic pulmonary fibrosis

Table of Contents

1. Introduction....3
2. Methods....6
2.1 Tissue Procurement and Preparation....6
2.2 Decellularization Protocols....7
2.3 Freeze-Dry and Weight Normalization....8
2.4 DNA Isolation and Quantification....8
2.5 Agarose Gel Electrophoresis....9
2.6 DAPI Staining....9
2.7 Total Protein Quantification....9
2.8 Sodium Dodecyl Sulfate Polyacrylamide Gel Electrophoresis (SDS-PAGE)....10
2.9 Soluble Collagen Assay....10
2.10 Insoluble Collagen Assay....11
2.11 Elastin Assay....11
2.12 Sulfated glycosaminoglycan (GAGs) Assay....11
2.13 Live/Dead Fluorescence Staining....11
2.14 Alamar Blue Assay....12
2.15 Statistical Analysis....13
3. Results....13
3.1 Decellularization success....13
3.2 Total Protein Changes....16
3.3 ECM Components....18
3.4 Cell Viability....24
3.5 Idiopathic Pulmonary Fibrosis....25
4. Discussion....29
5. Conclusion and Future Directions....33
References....35
Supplemental....37

1. Introduction

The extracellular matrix (ECM) is a dynamic three-dimensional network of proteins, glycoproteins, proteoglycans, and glycosaminoglycans that provide tissues with structural support while also regulating essential cellular functions [1]. The ECM does not just act as a passive scaffold, it actively supplies biochemical and mechanical cues that influence cell adhesion, migration, proliferation, differentiation, and survival, making it a central player for tissue homeostasis and repair [2]. Because ECM composition is produced and continuously remodeled by its resident cells, it is inherently tissue specific therefore each organ possesses a distinct matrix architecture and biochemical profile tailored to its essential functional needs. This reciprocal relationship between cells and matrix, described as dynamic reciprocity [3], is especially important in regenerative medicine because ECM-based biomaterials are becoming increasingly used to preserve or model native matrix composition, structure, and architecture in ways that simplified synthetic or single component systems often cannot [2], [4].

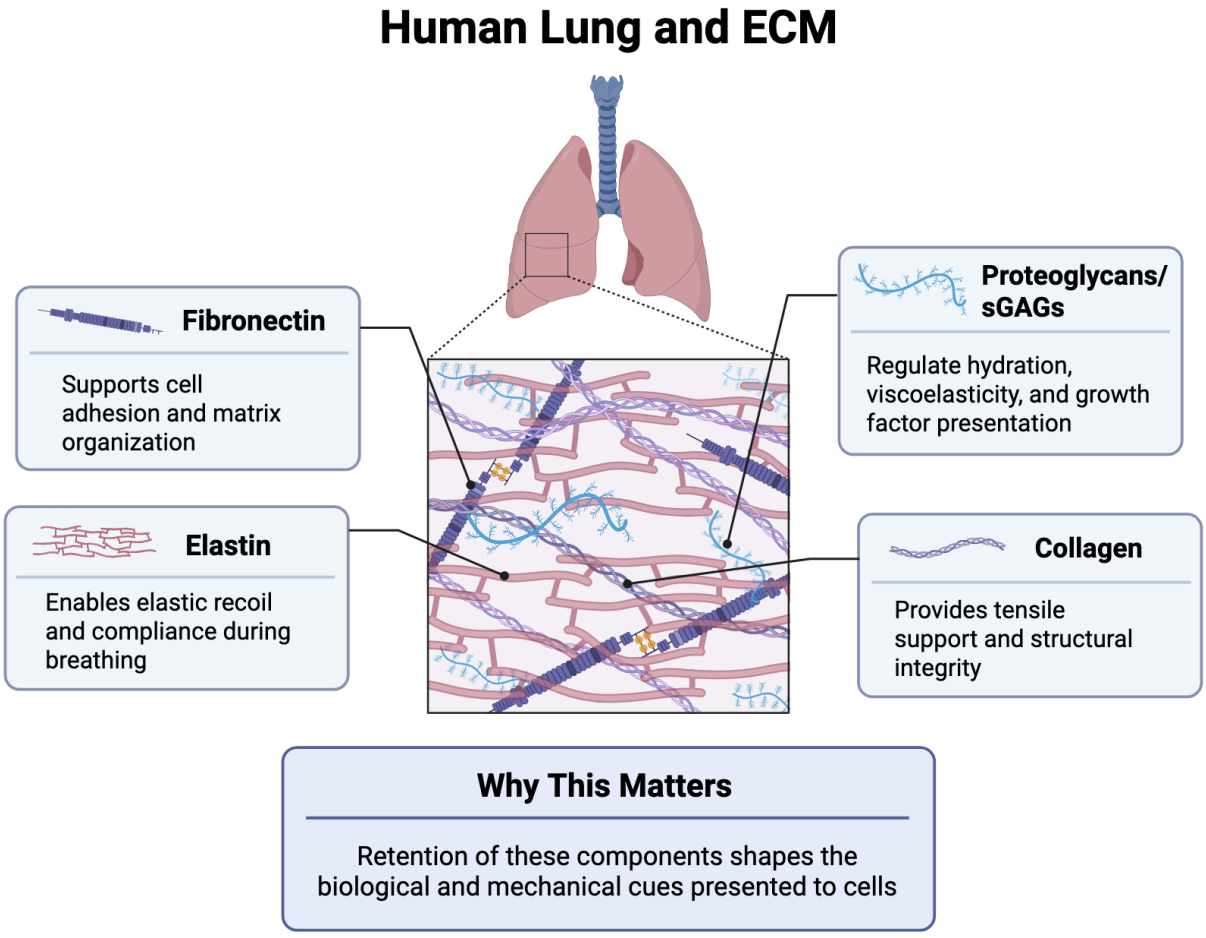


Figure 1. Human lung extracellular matrix (ECM) components and their primary roles in the lung microenvironment. Schematic of the human lung with a magnified view of the surrounding extracellular matrix, highlighting major ECM components relevant to this study, including fibronectin, elastin, collagen, and proteoglycans/sulfated glycosaminoglycans (sGAGs). These components contribute to cell adhesion, matrix organization, elastic recoil, tensile support, hydration, viscoelasticity, and growth factor presentation, and together help define the biological and mechanical cues experienced by resident lung cells.

These concepts are particularly important in the lung since the ECM must support a highly branched three-dimensional architecture of airways, vasculature, and alveoli while also maintaining the biochemical and mechanical conditions required for normal lung function [5]. Lung ECM contains major structural components, including laminin, collagen, fibronectin, proteoglycans, glycosaminoglycans, and elastin, which collectively contribute to barrier integrity, matrix signaling, and tissue recoil during breathing [5], [6]. Because the cells in the lung exist within this constantly changing 3D mechanically active environment, they respond to not only the matrix composition but also the matrix stiffness, viscoelasticity, degradability, and confinement through cell-ECM mechanotransductive pathways [1], [7]. This is especially important since mechanotransduction in 3D environments can greatly differ from mechanotransduction observed in conventional 2D culture systems that are typically employed in science [6], [8]. With this in mind, biomaterial platforms that better preserve the native lung matrix (especially in a 3D environment) become particularly attractive for studying pulmonary cell behavior in a more physiologically relevant context and for future mechanobiology applications [4], [5].

Decellularization has become a valuable method for producing lung biomaterials with these considerations in mind since it removes native cellular material while preserving an acellular matrix that more closely reflects the structural and biochemical complexities seen in the lungs [9], [10]. In the lung specifically, a decellularized matrix is attractive because it preserves the complex architecture, biomechanics, and topologic specificity of lung tissue, which is very difficult to reproduce using conventional fabrication methods or single component biomaterials [5]. In addition to preserving geometry, decellularized lung ECM can retain organ-specific extracellular matrix components that provide biologically relevant cues to seeded cells. Histologic and immunofluorescent analyses of decellularized lung scaffolds have shown preservation of key matrix proteins such as collagen, laminin, and fibronectin, all of which are important for epithelial attachment, endothelial support, and basement membrane associated signaling [5], [11]. Decellularized lung ECM is not only structurally preserved but also functionally useful as a substrate for pulmonary cell culture. Prior studies have shown that decellularized human, porcine, and mouse lung extracellular matrix can support attachment, viability, growth, and metabolic activity of multiple human cell types, including fibroblasts, small airway epithelial cells, and mesenchymal stem cells [12], [13], [14]. This makes decellularized lung ECM useful not only as a future transplantable scaffold concept but also as a practical in vitro biomaterial platform for studying cell-matrix interactions in a pulmonary-specific context. Therefore decellularized lung ECM is uniquely valuable for pulmonary biomaterials research as it preserves the native three dimensional framework of the lung, retains the organ-specific biochemical environment, and provides a scaffold capable of supporting cellular behavior [5], [9], [15].

Although decellularization produces one of the most physiologically relevant scaffolding methods, it is not a neutral processing variable since every cell removal strategy alters the ECM proteins to some extent while attempting to remove the cellular components. Therefore, the central challenge of decellularization is not simply maximal cell removal, but rather achieving an acceptable balance between removal of DNA and other immunogenic material and preservation of native ECM composition, microstructure, and mechanical properties [4], [5], [16]. Different classes of decellularization agents act through different mechanisms and as a result produce different types of matrix damage. Ionic, non-ionic, and zwitterionic

detergents all solubilize membranes effectively, but they differ much in how strongly they disrupt ECM proteins, glycosaminoglycan, basement membrane components, and overall tissue architecture [10], [17].

Among commonly used detergents, sodium dodecyl sulfate (SDS) is highly effective at removing nuclear and cytoplasmic material, but it also tends to denature proteins, disrupt microstructure, eliminate growth factors, and deplete matrix constituents such as glycosaminoglycans and basement membrane-associated proteins [10]. By contrast, less aggressive or differentially acting detergents such as Triton X-100 and CHAPS may better preserve certain structural features or matrix protein although they may be less effective in achieving complete decellularization depending on tissue thickness and cellularity [5], [17]. Importantly, the effect of a decellularization method is not determined by the reagent selected alone since concentration, duration of exposure, sequence of treatments, application method, and the physical characteristics of the tissue all influence the final biochemical and mechanical profile of the scaffold. This issue of trying to preserve as much matrix as possible in such a delicate 3D microstructure, such as the lung, becomes important when trying to optimize a decellularization protocol. In comparative studies of human and porcine lung extracellular matrix, different decellularization methods produced distinct retention patterns for major matrix components, with CHAPS showing better overall retention of many lung ECM proteins than SDS or a multistep detergent approach, while fibronectin and elastin were particularly sensitive to method-dependent loss [15]. O'Neill and colleagues also noted that the relationship between the retained ECM composition and scaffold mechanics may reflect the decellularization method itself rather than simply the absolute amount of individual matrix components remaining after processing. Therefore, these findings suggest that decellularization method can shape the biochemical identity of the final scaffold in ways that are highly relevant to downstream cell behavior, biomaterial performance, and interpretation of biological differences within the source tissue.

Biological sex is an important variable in lung biology because sex-related differences influence pulmonary development, immune responses, disease susceptibility, and clinical outcomes across the lifespan [18], [19]. Although sex differences are well recognized clinically in several respiratory diseases, recent pulmonary research statements have emphasized that sex is still not consistently incorporated into preclinical lung models, despite its potential to alter both mechanistic interpretation and translational relevance [20]. This problem is especially relevant when studying extracellular matrix biology, because sex-dependent differences have already been identified in matrix composition and remodeling in non-pulmonary tissues [21], [22], [23]. For instance, male and female tendon tissues in mice exhibit differences in morphology and selected biochemical features despite broadly similar mechanical properties [22], and male versus female valvular interstitial cells show distinct patterns of myofibroblastic activation, collagen production, matrix metalloproteinase expression, and metabolic activity during ECM remodeling [21]. Together these findings help support the idea that sex can influence matrix organization, matrix turnover, and cell–matrix interactions in ways that may not be apparent if tissues are analyzed without sex as a variable.

The relevance of sex as a biological variable is particularly important in idiopathic pulmonary fibrosis (IPF), a progressive fibrotic interstitial lung disease that shows clear sex based differences in progression and clinical presentation [24]. IPF is consistently male dominant across multiple registries and study cohorts and male sex has been associated with worse prognosis and outcomes. In addition, sex-associated differences in gene expression have been reported in IPF, including differential expression of genes linked

to matrix remodeling and fibrotic signaling such as MMP7 and CHI3L1, suggesting that biological sex may shape fibrotic pathways at the molecular level [25]. Despite this, the biochemical composition of decellularized human lung ECM has not been well characterized with sex as a biological variable, particularly in the context of how the decellularization processing conditions may themselves alter retained matrix content. Therefore, sex should be considered not only as a demographic descriptor, but as a biologically meaningful factor that may influence the matrix environment used for downstream biomaterial development, disease modeling, and future mechanobiology studies.

Despite growing interest in using decellularized lung biomaterials, the biochemical characterization of human lung dECM remains limited, especially in studies that evaluate both sex as a biological variable and decellularization method within the same experimental framework. The need for this study is important because prior lung decellularization studies have shown that processing method can change retained collagen, sulfated glycosaminoglycans, elastin, fibronectin, and overall scaffold mechanics, showing that the final matrix profile reflects not only the source tissue but also how that tissue is processed [14]. Therefore, the objective of this thesis is to compare two human lung decellularization methods, evaluate efficacy, and characterize retained total protein and key extracellular matrix components in native and decellularized tissues with sex based stratification. This thesis also includes preliminary IPF samples as a step towards understanding how disease state may interact with matrix composition and scaffold design and see how the composition of diseased lung compares to healthy. The hypothesis of this study is that retained human lung ECM composition would differ by sex, but that these differences would also be shaped by decellularization method, therefore method dependent ECM retention would be a critical factor of the final biochemical environment of the scaffold.

2. Methods

2.1 Tissue Procurement and Preparation

Human lung tissue samples were obtained through a material transfer agreement with the Ballenger Lab at The Ohio State University through the Comprehensive Transplant Center at the OSU Wexner Medical Center. All tissues were collected and assessed by the Transplant Center prior to laboratory use. Lung tissues were obtained from both healthy donors and donors diagnosed with idiopathic pulmonary fibrosis (IPF). The study cohort included healthy male (n = 5), healthy female (n = 3), IPF male (n = 1), and IPF female (n = 1) samples. Donor demographics, including age and sex, are summarized in TABLE 1. Lung tissues were stored at -80 °C until further processing.

Table 1. Human Lung Donor Demographics

Sample Number	Condition	Sex	Age (years)
001	IPF	M	57
002	IPF	F	64
003	Healthy	M	53
004	Healthy	M	42
005	Healthy	M	29
006	Healthy	F	50
007	Healthy	F	71
008	Healthy	F	50
009	Healthy	M	64
010	Healthy	M	42

2.2 Decellularization Protocols

Human lung tissues were decellularized using detergent-based protocols designed to remove cellular components while preserving extracellular matrix (ECM) structure. Two decellularization conditions were evaluated to assess the effect of detergent concentration on ECM retention: a 0.1% sodium dodecyl sulfate (SDS) protocol and a 0.5% SDS protocol and will be named to and referred to as so throughout the paper. All other processing steps were identical between conditions.

Prior to decellularization, frozen tissue samples were thawed at 4 °C and mechanically processed into 3-5 mm fragments using sterile scissors. Care was taken to isolate parenchymal lung tissue and exclude large airway structures such as the trachea, bronchi, and any cartilage. Processed tissue samples were portioned into approximately 5 g portions. Samples were transferred to sterile 1 L duran bottles and processed under constant agitation on an orbital shaker (200 rpm) (New Brunswick™ Excella® E24 Incubator Shaker, Eppendorf) at room temperature (20–22 °C) for all steps unless otherwise specified.

Tissues were first rinsed in sterile 1× phosphate-buffered saline (PBS, Gibco™, Cat. No. 14040133) for 30 minutes to remove residual blood and debris, followed by a 30-minute rinse in deionized water (dH_2O) to induce osmotic lysis. Samples were then incubated in 0.1% (v/v) Triton X-100 (Thermo Fisher, Cat. No. ICN19485450) for 24 hours to solubilize lipid membranes. Following Triton treatment tissues were rinsed in dH_2O for 30 minutes. Samples were then subjected to SDS (Millipore Sigma, Cat. No. 151-21-3) treatment for 24 hours to facilitate removal of nuclear and cytoplasmic material. For this step, tissues were exposed to either 0.1% (w/v) SDS or 0.5% (w/v) SDS, depending on the experimental group. After SDS treatment, tissues were rinsed in dH_2O for 30 minutes to remove residual detergent. Samples were then washed in 1× PBS for 24 hours to ensure thorough removal of residual reagents. The tissues were then washed again in dH_2O for 30 minutes and then followed by a 1 hour final sterile 1× PBS wash. Following completion of the decellularization process, tissues were transferred to sterile conical tubes and stored in fresh 1× PBS. Samples were stored at −80 °C for long-term storage.

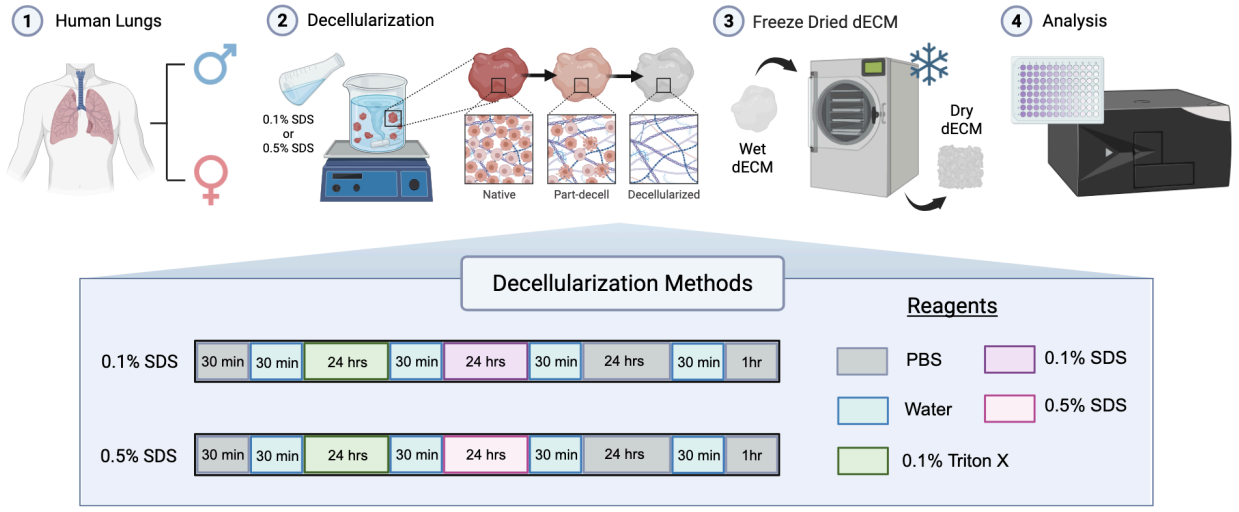


Figure 2. Schematic of the human lung decellularization and downstream analysis workflow. Human lung tissues from male and female donors were processed using detergent-based decellularization protocols containing either 0.1% SDS or 0.5% SDS. Tissues progressed from native to partially decellularized and fully decellularized extracellular matrix (dECM), after which samples were freeze-dried to enable both wet- and dry-weight normalization for downstream assays. The bottom panel outlines the reagent sequence and exposure durations used during decellularization, consisting of PBS rinses, water washes, Triton X-100 treatment, SDS treatment, and final wash steps. Both protocols were identical except for SDS concentration.

2.3 Freeze-Dry and Weight Normalization

Following decellularization, tissue samples were subjected to lyophilization to remove water content and enable standardized comparison of extracellular matrix (ECM) composition. Samples were frozen and dried using a commercial freeze dryer (Harvest Right, USA) for approximately 24 hours, or until complete dehydration was achieved. All biochemical assays were performed using both wet and dry weight normalization to evaluate the impact of decellularization on ECM composition relative to tissue mass. This approach allowed for comparison of results independent of variations in water content introduced during processing.

2.4 DNA Isolation and Quantification

DNA was isolated from both native and decellularized human lung tissue using the GeneJET Genomic DNA Purification Kit (Thermo Fisher Scientific, Cat. No. K0721). For each sample, approximately 20 mg of tissue (normalized by wet or dry weight, as specified) was transferred to a 1.5 mL microcentrifuge tube. To each sample, 180 µL of digestion solution and 20 µL of Proteinase K were added. Samples were vortexed for 30 seconds to ensure uniform suspension and then incubated overnight at 56 °C to achieve complete tissue digestion. Following digestion, samples were processed according to the manufacturer's instructions to isolate genomic DNA.

Purified DNA was either used immediately for downstream applications or stored at −20 °C until further analysis. DNA concentration and purity were measured by absorbance at 260 nm and 280 nm using a Thermo Scientific™ NanoDrop™ One spectrophotometer (Thermo Fisher Scientific). DNA content was

normalized to tissue mass and reported as nanograms of DNA per milligram of tissue (ng/mg) for both wet and dry weight conditions.

2.5 Agarose Gel Electrophoresis

A 2% (w/v) agarose gel was prepared by dissolving 2 g of agarose (Millipore Sigma, Cat. No. A6013-25G) in 100 mL of 1× Tris-acetate-EDTA (TAE) buffer (Bio-Rad, Cat. No. 1610773). The solution was heated in a microwave for approximately 1 minute until the agarose was fully dissolved and then allowed to cool to a warm temperature prior to the addition of 8 µL of SYBR Safe DNA gel stain (Thermo Fisher Scientific, Cat. No. S33102) for DNA visualization. The agarose solution was poured into a gel casting tray (15 × 7 cm, Bio-Rad, Cat. No. 1704426), and a comb was inserted to form wells. The gel was allowed to solidify at room temperature for approximately 30–40 minutes.

DNA samples from native and decellularized human lung tissues were prepared by mixing with 6× Cyan/Orange loading dye (Thermo Fisher Scientific, Cat. No. 10482028). For each sample, 100 ng of DNA was combined with loading dye and deionized water to achieve a total volume of 20 µL. Once solidified, the gel was placed into an electrophoresis chamber (Bio-Rad, Cat. No. 1704484) and submerged in 1× TAE buffer. Prepared samples were loaded into the wells, along with a 100 bp DNA ladder (Thermo Fisher Scientific, Cat. No. SM0243) to enable size comparison. Electrophoresis was performed at 80 V for approximately 60 minutes. Following electrophoresis, gels were imaged using a ChemiDoc™ Imaging System (Bio-Rad). This analysis was used to assess DNA fragmentation and confirm effective decellularization.

2.6 DAPI Staining

DAPI staining was performed to qualitatively assess the presence of residual nuclei in native and decellularized human lung tissues following processing. Approximately 20 mg of tissue was rinsed in 1× phosphate-buffered saline (PBS) and fixed in 4% paraformaldehyde (PFA) for 15–20 minutes at room temperature. Following fixation, samples were washed three times with 1× PBS. A DAPI stock solution was prepared from DAPI powder (Invitrogen™, Thermo Fisher Scientific, Cat. No. D1306) at 5 mg/mL by dissolving the contents of the vial in deionized water according to the manufacturer's recommendations. A working solution was then prepared at 1 µg/mL in PBS. Tissues were incubated in the DAPI working solution for 10 minutes at room temperature, protected from light, followed by PBS washes to remove excess stain. Samples were then imaged using an EVOS™ M3000 Imaging System (Thermo Fisher Scientific) at 10× magnification using the DAPI fluorescence channel.

2.7 Total Protein Quantification

Total protein content was quantified to evaluate extracellular matrix (ECM) retention following decellularization. Proteins were extracted from approximately 50 mg of native and decellularized human lung tissue using radioimmunoprecipitation assay (RIPA) buffer (Thermo Fisher Scientific, Cat. No. PI89900) supplemented with 1× HALT protease inhibitor cocktail (Thermo Fisher Scientific, Cat. No. PI87786).

Briefly, tissue samples were homogenized in 198 µL of 1× RIPA buffer and 2 µL of 100× protease inhibitor using a handheld homogenizer (Benchmark Scientific, Model D1000) for 30 seconds, followed by 30 seconds on ice. This homogenization cycle was repeated three times to ensure complete tissue disruption while minimizing sample overheating. Samples were then incubated on ice for 1 hour to facilitate protein extraction. Following incubation, samples were centrifuged at 14,000 × g for 20 minutes at 4 °C. The resulting supernatant containing solubilized proteins was collected and either used immediately or stored at −20 °C until further analysis.

Total protein concentration was determined using a bicinchoninic acid (BCA) assay kit (Thermo Fisher Scientific, Cat. No. 23225) according to the manufacturer's protocol. The working reagent was prepared by combining Reagent A and Reagent B at a 50:1 ratio. For each sample, 25 µL of protein extract was mixed with 200 µL of working reagent in a 96-well plate and gently agitated for 30 seconds. The plate was then incubated at 37 °C for 30 minutes. Absorbance was measured at 562 nm using a microplate reader (Infinite 200 PRO, Tecan), and protein concentration was calculated based on a standard curve. Protein content was normalized to tissue mass and reported for both wet and dry weight conditions.

2.8 Sodium Dodecyl Sulfate Polyacrylamide Gel Electrophoresis (SDS-PAGE)

Sodium dodecyl sulfate polyacrylamide gel electrophoresis (SDS-PAGE) was performed to evaluate protein profiles in native and decellularized human lung tissues. Protein concentrations were first determined (Section 2.7), and loading amounts were adjusted to 10 µg for each sample per well.

Protein samples were prepared by mixing 2× Laemmli sample buffer (Bio-Rad, Cat. No. 1610737) and 5% (v/v) β-mercaptoethanol (Sigma-Aldrich, Cat. No. M6250). Samples were then heated at 90 °C for 10 minutes to denature proteins. Denatured proteins were separated on 4–15% gradient Mini-PROTEAN® TGX™ gels (Bio-Rad, Cat. No. 4561023) alongside a pre-stained protein ladder (PageRuler™ Plus, Thermo Fisher Scientific, Cat. No. 26621). Electrophoresis was conducted at a constant voltage of 80 V for approximately 90 minutes. Following separation, gels were stained with Coomassie Brilliant Blue (Thermo Fisher Cat. No. 20279) to visualize protein bands. Images were captured using a ChemiDoc™ Imaging System (Bio-Rad) for qualitative assessment of protein presence and distribution.

2.9 Soluble Collagen Assay

Soluble collagen content was quantified to assess ECM composition before and after decellularization. A Sircol™ Soluble Collagen Assay kit (Biocolor Ltd., Cat. No. 502120-046) was used according to the manufacturer's instructions. 20 mg of native and decellularized human lung tissue was digested in pepsin (Sigma Aldrich, Cat. No. P7012) solution (0.1 mg/mL in 0.5 M acetic acid (Thermo Fisher Cat. No. A38212)) at 4 °C overnight under continuous agitation on a mechanical shaker to extract soluble collagen.

Following digestion, samples were centrifuged at 3,000 × g for 10 minutes to separate insoluble material. The resulting supernatant containing solubilized collagen was collected and processed according to the assay protocol. Absorbance was measured at 556 nm using a microplate reader (Infinite 200 PRO, Tecan), and collagen concentration was determined based on a standard curve provided with the kit. Collagen content was normalized to tissue mass and reported for both wet and dry weight conditions.

2.10 Insoluble Collagen Assay

Insoluble collagen content was quantified to further assess ECM composition before and after decellularization. A Sircol™ Insoluble Collagen Assay kit (Biocolor Ltd., Cat. No. 103737-182) was used according to the manufacturer's instructions. 20 mg of native and decellularized human lung tissue was digested in 1 mL of fragmentation reagent and incubated at 65 °C for 3 hours to solubilize insoluble collagen components.

Following digestion, samples were centrifuged at 13,000 × g for 10 minutes to remove remaining debris. The resulting supernatant was collected and processed according to the assay protocol. Absorbance was measured at 556 nm using a microplate reader (Infinite 200 PRO, Tecan), and collagen concentration was determined based on a standard curve provided with the kit. Collagen content was normalized to tissue mass and reported for both wet and dry weight conditions.

2.11 Elastin Assay

Elastin content was quantified to assess ECM composition following decellularization. A Fastin™ Elastin Assay kit (Biocolor Ltd., Cat. No. 104026-102) was used according to the manufacturer's instructions. 20 mg of native and decellularized human lung tissue was digested in 750 µL of 0.25 M oxalic acid and incubated at 100 °C for 3 hours to solubilize elastin components.

Following digestion, samples were centrifuged at 13,000 × g for 10 minutes to remove insoluble debris. The resulting supernatant was collected and processed according to the assay protocol. Absorbance was measured at 513 nm using a microplate reader (Infinite 200 PRO, Tecan), and elastin concentration was determined based on a standard curve provided with the kit. Elastin content was normalized to tissue mass and reported for both wet and dry weight conditions.

2.12 Sulfated glycosaminoglycan (GAGs) Assay

Sulfated glycosaminoglycan (sGAG) content was quantified to assess ECM composition for native and decellularized tissues. A Blyscan™ Glycosaminoglycan Assay kit (Biocolor Ltd., Cat. No. 501725937) was used according to the manufacturer's instructions. 50 mg of native and decellularized human lung tissue was digested in 1 mL of papain extraction reagent and incubated at 65 °C for 3 hours to release sulfated glycosaminoglycans.

Following digestion, samples were centrifuged at 10,000 × g for 10 minutes to remove insoluble debris. The resulting supernatant was collected and processed according to the assay protocol. Absorbance was measured at 656 nm using a microplate reader (Infinite 200 PRO, Tecan), and sGAG concentration was determined based on a standard curve provided with the kit. sGAG content was normalized to tissue mass and reported for both wet and dry weight conditions.

2.13 Live/Dead Fluorescence Staining

Cell viability was evaluated using conditioned media derived from decellularized human lung tissue. Conditioned media was prepared by incubating 10 mg of dECM in complete cell culture medium consisting of Dulbecco's Modified Eagle Medium (DMEM, Gibco, Cat. No. 11965092), supplemented

with 10% fetal bovine serum (Fisherbrand, Cat. No. FB12999102) and 1× antibiotic-antimycotic (Gibco, Cat. No. 15240112). The mixture was incubated for 3 days to allow for release of soluble factors from the dECM.

NIH 3T3 fibroblast cells were seeded at a density of 3,000 cells per well in a 96-well plate and cultured in conditioned media derived from decellularized tissues. Control samples were maintained in standard culture media without dECM conditioning. Cells were cultured for 3 days, with imaging performed daily to monitor cell viability.

Live/Dead staining was performed using calcein AM (Invitrogen™, Cat. No. C1430) and propidium iodide (Millipore Sigma, Cat. No. P4170) to distinguish viable and non-viable cells. Cells were incubated with 2 μM calcein AM and 1 μg/mL propidium iodide at 37 °C for 20 minutes, protected from light. Following incubation, cells were imaged immediately using an EVOS™ M3000 Imaging System (Thermo Fisher Scientific) at 10× magnification. Fluorescence images were analyzed using a custom MATLAB script to quantify live (green) and dead (red) cells. Cell viability was calculated as the percentage of live cells relative to the total cell count.

In addition to conditioned-media experiments, Live/Dead fluorescence imaging was also performed following direct culture of NIH 3T3 fibroblasts on human dECM tissue. After completion of the 3-day direct-contact culture period used for the Alamar Blue assay, tissues were stained using the same Live/Dead staining solution and incubation conditions described above, consisting of 2 μM calcein AM and 1 μg/mL propidium iodide for 20 minutes at 37 °C protected from light. Stained tissues were then imaged using an EVOS™ M3000 Imaging System (Thermo Fisher Scientific) at 10× magnification to qualitatively assess cell viability and attachment on the dECM surface.

2.14 Alamar Blue Assay

Metabolic activity was assessed using the alamarBlue™ Cell Viability Reagent (Invitrogen™, Thermo Fisher Scientific; Cat. No. DAL1025) to evaluate cell viability following direct contact with dECM. NIH 3T3 fibroblasts were seeded at a density of 30,000 cells per well in a 48-well plate containing human dECM tissue samples. On Day 0, cells were seeded onto the tissues in 500 μL of cell suspension per well. On Day 1, an optimization study was performed to determine the appropriate alamarBlue incubation period for the following measurements (Figure S1). Each well was brought to a total volume of 1,000 μL by adding 400 μL of fresh complete culture medium and 100 μL of alamarBlue reagent, corresponding to a 1X working concentration from the 10X stock reagent. Samples were incubated at 37 °C, and 100 μL aliquots were transferred hourly over a 4-hour period into a 96-well plate for absorbance measurement. At the end of the optimization study, medium was removed and replaced with 500 μL of fresh complete medium.

On Days 2 and 3, 50 μL of alamarBlue reagent was added directly to each well containing 500 μL of culture medium (1X working concentration). Samples were incubated for the optimized duration of 4 hours as determined from the Day 1 time-course experiment. Following incubation, 100 μL aliquots were transferred to a 96-well plate and absorbance was measured at 570 nm and 600 nm using a microplate reader. Metabolic activity was used as an indicator of cell viability following direct dECM exposure.

2.15 Statistical Analysis

All statistical analyses were performed using GraphPad Prism version 10.4.0 (GraphPad Software). For the healthy human tissue datasets, biological replicates were defined at the donor level. When technical replicates were collected, values were first averaged within each donor prior to statistical testing. Quantitative data for healthy donor comparisons are presented as mean ± standard error of the mean (SEM).

To evaluate the effects of decellularization condition and sex on DNA content, total protein, extracellular matrix (ECM) component content, and viability-related outcomes, two-way mixed-effects models (REML) were used. In these analyses, condition (native, 0.1% SDS, and 0.5% SDS) was treated as the repeated measure within donor, and sex was treated as a between-subject factor. When significant main effects or interactions were identified, Šídák multiple-comparisons tests were performed as appropriate. A value of $p < 0.05$ was considered statistically significant.

For exploratory comparison of the preliminary IPF dataset, unpaired parametric t-tests with Welch's correction were performed on technical replicate values within each donor group. Because these analyses were based on technical replicates from n = 1 donor per sex, resulting p-values are presented for exploratory purposes only and should not be interpreted as definitive biological inference.

3. Results

3.1 Decellularization success

Human lung tissue was successfully decellularized under both SDS conditions, as demonstrated by substantial reductions in residual DNA content together with loss of visible nuclear material and reduced DNA banding (Figure 3). Quantitative DNA analysis showed that residual DNA content was significantly reduced in decellularized tissues compared to native tissues under both wet- and dry-weight normalization (Figure 3A; Table 2). Under wet-weight normalization, male native tissue contained 496.62 ± 56.77 ng/mg DNA, which decreased to 23.32 ± 5.08 ng/mg in the 0.1% SDS group and 38.10 ± 4.41 ng/mg in the 0.5% SDS group. Female native tissue contained 284.09 ± 167.43 ng/mg DNA, which decreased to 49.98 ± 9.35 ng/mg following 0.1% SDS treatment and 24.58 ± 10.17 ng/mg following 0.5% SDS treatment. These values corresponded to reductions of 95.30% and 92.33% in male tissues and 82.41% and 91.35% in female tissues for the 0.1% and 0.5% SDS conditions, respectively.

A similar trend was observed under dry-weight normalization, further supporting effective decellularization. Male native tissue contained 342.83 ± 97.91 ng/mg DNA, which decreased to 20.57 ± 3.89 ng/mg in the 0.1% SDS group and 36.25 ± 3.22 ng/mg in the 0.5% SDS group. Female native tissue contained 106.72 ± 41.35 ng/mg DNA, which decreased to 60.17 ± 11.42 ng/mg after 0.1% SDS treatment and 34.19 ± 2.78 ng/mg after 0.5% SDS treatment. These corresponded to reductions of 94.00% and 89.43% in male tissues and 43.62% and 67.97% in female tissues for the 0.1% and 0.5% SDS conditions, respectively. Importantly, dry-weight residual DNA values in male 0.1% SDS, male 0.5% SDS, female 0.1% SDS, and female 0.5% SDS tissues were below the commonly cited 50 ng/mg threshold used to indicate sufficient decellularization. When stratified by sex, both male and female

decellularized tissues still showed markedly lower residual DNA content than their corresponding native tissues, supporting substantial removal of cell-associated material under both protocols.

Table 2. Residual DNA content in human lung tissue normalized to wet and dry weight. Data are presented as mean ± SEM based on donor-averaged values. Male native groups were calculated from n = 5 donors and female native groups from n = 3 donors.

Normalization	Sex	Native (ng/mg)	0.1% SDS dECM (ng/mg)	0.5% SDS dECM (ng/mg)	% Reduction (0.1% SDS)	% Reduction (0.5% SDS)
Wet weight	Male	496.62 ± 56.77	23.32 ± 5.08	38.10 ± 4.41	95.30%	92.33%
Wet weight	Female	284.09 ± 167.43	49.98 ± 9.35	24.58 ± 10.17	82.41%	91.35%
Dry weight	Male	342.83 ± 97.91	20.57 ± 3.89	36.25 ± 3.22	94.00%	89.43%
Dry weight	Female	106.72 ± 41.35	60.17 ± 11.42	34.19 ± 2.78	43.62%	67.97%

Qualitative nuclear staining further supported these findings. Representative DAPI images showed abundant nuclear staining in native male and female tissues, whereas both the 0.1% SDS and 0.5% SDS decellularized tissues exhibited minimal to no visible nuclear signal (Figure 3B). These images indicate the substantial removal of cell associated nuclear material following decellularization.

Agarose gel electrophoresis provided additional confirmation of DNA removal and fragmentation. Native tissues displayed strong high-molecular weight DNA bands (red boxes) while decellularized tissues showed reduced overall band intensity (Figure 3C). Minimal visible signal was observed in the sub-200 bp region (yellow boxes) in the decellularized groups, which is consistent with reduced residual DNA fragmentation after detergent treatment. Altogether, the quantitative and qualitative assessments shown in Figure 3 support successful decellularization of human lung tissue under both SDS conditions.

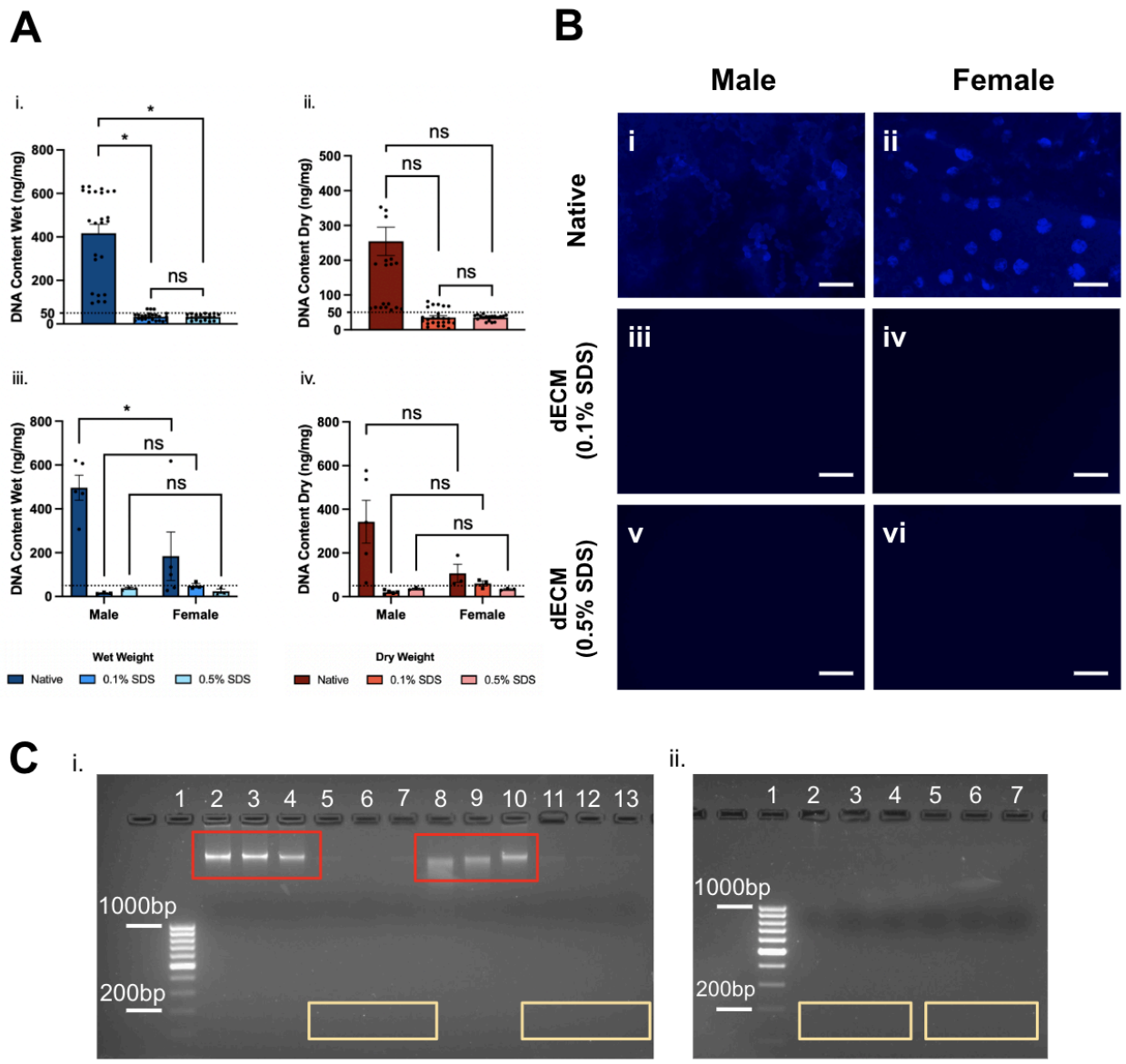


Figure 3. Quantification of DNA content in native and decellularized human extracellular matrix (dECM) tissues. (A) Quantification of DNA content expressed per (i) wet weight without stratification by sex and (ii) dry weight without stratification by sex, comparing native, 0.1% SDS, and 0.5% SDS conditions. (iii) DNA content expressed per wet weight with sex-based stratification and (iv) per dry weight with sex-based stratification. (B) Representative nuclear staining images (DAPI) of native and dECM tissues from male and female samples, demonstrating removal of cellular nuclei following decellularization. Scale bar = 100 µm. (C) Representative agarose gel electrophoresis images assessing DNA integrity in native and decellularized human lung tissues. (i) Lane 1: DNA ladder; lanes 2–4: male native; lanes 5–7: male dECM (0.1% SDS); lanes 8–10: female native; lanes 11–13: female dECM (0.1% SDS). (ii) Lane 1: DNA ladder; lanes 2–4: male dECM (0.5% SDS); lanes 5–7: female dECM (0.5% SDS). Red boxes highlight strong high-molecular-weight DNA signal in native tissues, while yellow boxes indicate the sub-200 bp region used to assess DNA fragmentation following decellularization. Minimal visible signal in this lower region, together with reduced overall DNA banding in dECM samples, is consistent with effective decellularization. Data are presented as mean ± SEM (n = 5 for male, n = 3 for female). Statistical significance is denoted as ****$p \leq 0.0001$, ***$p \leq 0.001$, **$p \leq 0.01$, and *$p \leq 0.05$.

3.2 Total Protein Changes

Total protein content following decellularization was assessed using BCA quantification and SDS-PAGE to evaluate both quantitative changes in protein content and qualitative differences in protein banding patterns (Figure 4). In the non-sex-stratified analysis, total protein content was significantly reduced in decellularized tissues compared to native tissues under both wet- and dry-weight normalization (Figure 4A). Under wet-weight normalization, total protein content was significantly reduced following decellularization (Figure 4A; Table 3). Male native tissue contained 10559.61 ± 849.14 ng/mg total protein, which decreased to 908.92 ± 178.27 ng/mg in the 0.1% SDS group and 947.00 ± 218.27 ng/mg in the 0.5% SDS group. Female native tissue contained 9071.77 ± 58.82 ng/mg total protein, which decreased to 1246.53 ± 225.34 ng/mg following 0.1% SDS treatment and to 960.18 ± 60.05 ng/mg following 0.5% SDS treatment. These corresponded to protein retention values of 8.61% and 8.97% in male tissues and 13.74% and 10.58% in female tissues for the 0.1% and 0.5% SDS conditions, respectively. Mixed-effects analysis demonstrated a significant main effect of condition on wet-weight normalized total protein content ($p < 0.0001$). Post hoc comparisons of the overall condition means showed that both the 0.1% SDS and 0.5% SDS groups were significantly lower than native tissue (both $p < 0.0001$). Within male tissues, native protein content was significantly higher than both male 0.1% SDS ($p = 0.0072$) and male 0.5% SDS ($p = 0.0021$). Similarly, within female tissues, native protein content was significantly higher than both female 0.1% SDS ($p = 0.0024$) and female 0.5% SDS ($p < 0.0001$).

A similar overall trend was observed under dry-weight normalization, with total protein content remaining substantially lower in both decellularized groups than in native tissue (Figure 4A; Table 3). Male native tissue contained 10368.59 ± 115.85 ng/mg total protein, which decreased to 3206.70 ± 500.96 ng/mg in the 0.1% SDS group and 2452.58 ± 747.29 ng/mg in the 0.5% SDS group. Female native tissue contained 10024.21 ± 382.94 ng/mg total protein, which decreased to 3794.50 ± 1230.67 ng/mg after 0.1% SDS treatment and 2742.00 ± 329.53 ng/mg after 0.5% SDS treatment. These corresponded to protein retention values of 30.93% and 23.65% in male tissues and 37.85% and 27.35% in female tissues for the 0.1% and 0.5% SDS conditions, respectively. Mixed-effects analysis demonstrated a significant main effect of condition on dry-weight normalized total protein content ($p < 0.0001$). Post hoc comparisons of the overall condition means showed that both the 0.1% SDS and 0.5% SDS groups were significantly lower than native tissue (both $p < 0.0001$), whereas no significant difference was detected between the 0.1% SDS and 0.5% SDS groups ($p = 0.6353$). Within-sex comparisons showed that male native tissue remained significantly higher than both male 0.1% SDS ($p = 0.0002$) and male 0.5% SDS ($p = 0.0399$), while female native tissue was significantly higher than female 0.5% SDS ($p = 0.0022$).

Table 3. Total protein content in human lung tissue normalized to wet and dry weight. Data are presented as mean ± SEM based on donor-averaged values. Male native groups were calculated from n = 5 donors and female native groups from n = 3 donors.

Normalization	Sex	Native (ng/mg)	0.1% SDS dECM (ng/mg)	0.5% SDS dECM (ng/mg)	% Retention (0.1% SDS)	% Retention (0.5% SDS)
Wet weight	Male	10559.61 ± 849.14	908.92 ± 178.27	947.00 ± 218.27	8.61%	8.97%
Wet weight	Female	9071.77 ± 58.82	1246.53 ± 225.34	960.18 ± 60.05	13.74%	10.58%
Dry weight	Male	10368.59 ± 115.85	3206.70 ± 500.96	2452.58 ± 747.29	30.93%	23.65%
Dry weight	Female	10024.21 ± 382.94	3794.50 ± 1230.67	2742.00 ± 329.53	37.85%	27.35%

Qualitative protein analysis by SDS-PAGE further supported these findings. Native tissues showed stronger and more broadly distributed protein banding patterns than decellularized tissues, indicating greater overall protein presence prior to processing. Protein bands remained detectable in both the 0.1% SDS and 0.5% SDS decellularized samples, confirming that residual proteins were retained after decellularization, although band intensity was visibly reduced relative to native tissue. The 0.1% SDS samples also exhibited stronger banding than the 0.5% SDS samples, which is consistent with the quantitative BCA findings showing greater protein retention with the 0.1% SDS method. Overall, the quantitative and qualitative assessments in Figure 4 demonstrate substantial protein loss following decellularization while also supporting method-dependent differences in retained protein content.

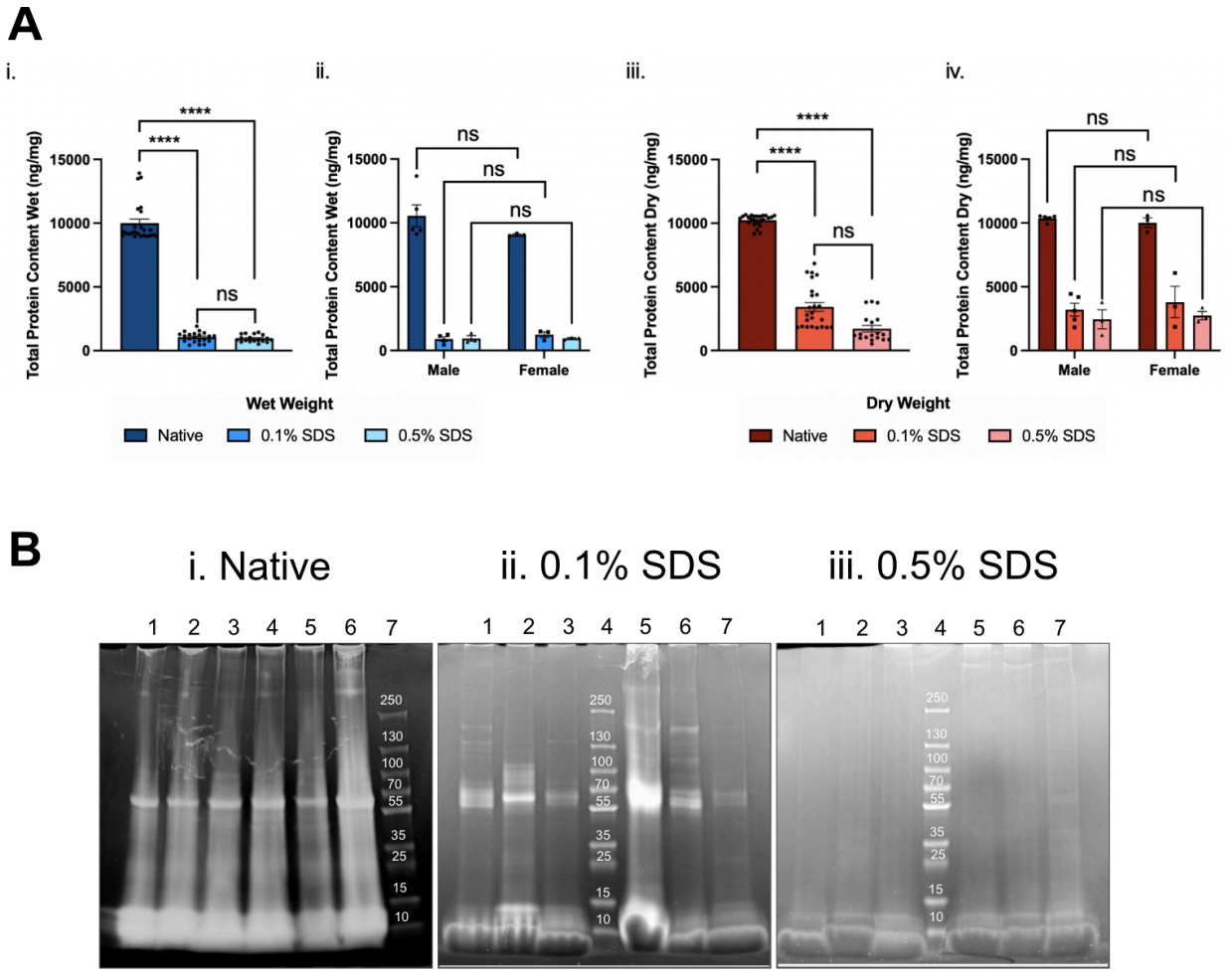


Figure 4. Quantification of total protein content in native and decellularized human extracellular matrix (dECM) tissues. (A) Quantification of total protein content expressed per (i) wet weight without stratification by sex and (ii) wet weight with stratification by sex, comparing native, 0.1% SDS, and 0.5% SDS conditions. (iii) Total protein content expressed per dry weight without sex-based stratification and (iv) per dry weight with sex-based stratification. (B) Representative SDS-PAGE analysis of protein profiles in native and decellularized human lung tissues. (i) Native tissue: lanes 1–3, male native; lanes 4–6, female native; lane M, protein ladder. (ii) 0.1% SDS dECM: lanes 1–3, male dECM; lane M, protein ladder; lanes 5–7, female dECM. (iii) 0.5% SDS dECM: lanes 1–3, male dECM; lane M, protein ladder; lanes 5–7, female dECM. Molecular weight standards are indicated in kDa. Data are presented as mean ± SEM (n = 5 for male, n = 3 for female). Statistical significance is denoted as ****$p \leq 0.0001$, ***$p \leq 0.001$, **$p \leq 0.01$, and *$p \leq 0.05$.

3.3 ECM Components

Retention of specific ECM components following decellularization was evaluated by quantifying insoluble collagen, soluble collagen, elastin, and sulfated glycosaminoglycans (sGAG) in native and decellularized human lung tissues. Measurements were normalized to both wet and dry tissue weight and are summarized in Figure 5 and Table 4, while the corresponding relative ECM composition profiles are shown in Figure 6. Together, these analyses demonstrate that decellularization altered both the absolute amount and the proportional balance of the measured ECM components, with differences observed between the 0.1% SDS and 0.5% SDS treatment groups as well as between male and female tissues.

Table 4. ECM component content in human lung tissue normalized to wet and dry weight.

ECM Component	Normalization	Sex	Native (ng/mg)	0.1% SDS dECM (ng/mg)	0.5% SDS dECM (ng/mg)	% Retention (0.1% SDS)	% Retention (0.5% SDS)
Insoluble Collagen	Wet weight	Male	2929.07 ± 166.18	1380.93 ± 119.75	887.78 ± 68.49	47.15%	30.31%
	Wet weight	Female	2463.56 ± 540.09	2100.00 ± 458.77	822.00 ± 244.81	85.24%	33.37%
	Dry weight	Male	36328.00 ± 9136.07	21340.67 ± 3474.41	5426.89 ± 293.53	58.74%	14.94%
	Dry weight	Female	36691.33 ± 6656.19	21467.78 ± 2704.12	4809.11 ± 1814.18	58.51%	13.11%
Soluble Collagen	Wet weight	Male	3232.11 ± 705.22	1023.02 ± 256.41	183.42 ± 44.84	31.65%	5.65%
	Wet weight	Female	2398.66 ± 83.18	1382.81 ± 233.97	307.61 ± 68.90	57.65%	12.82%
	Dry weight	Male	13727.68 ± 1636.38	1736.85 ± 887.20	575.90 ± 138.69	12.65%	4.20%
	Dry weight	Female	8509.53 ± 334.99	2392.65 ± 95.39	1545.90 ± 516.51	28.12%	18.17%
Elastin	Wet weight	Male	3085.90 ± 726.81	952.60 ± 42.62	592.83 ± 5.55	30.87%	19.21%
	Wet weight	Female	1563.17 ± 139.54	981.50 ± 253.33	597.67 ± 53.36	62.79%	38.23%
	Dry weight	Male	19390.60 ± 2200.76	10076.70 ± 1879.20	2443.80 ± 157.57	51.97%	12.60%
	Dry weight	Female	22866.33 ± 1633.56	10575.50 ± 1927.15	2276.85 ± 223.07	46.25%	9.96%
sGAG	Wet weight	Male	268.40 ± 41.83	26.93 ± 3.34	2.17 ± 0.82	10.03%	0.81%
	Wet weight	Female	388.64 ± 15.15	27.76 ± 2.01	2.51 ± 0.88	7.14%	0.64%
	Dry weight	Male	298.39 ± 26.34	107.21 ± 32.68	88.32 ± 58.16	35.93%	29.60%
	Dry weight	Female	345.78 ± 12.54	68.17 ± 11.06	13.80 ± 9.92	19.72%	3.99%

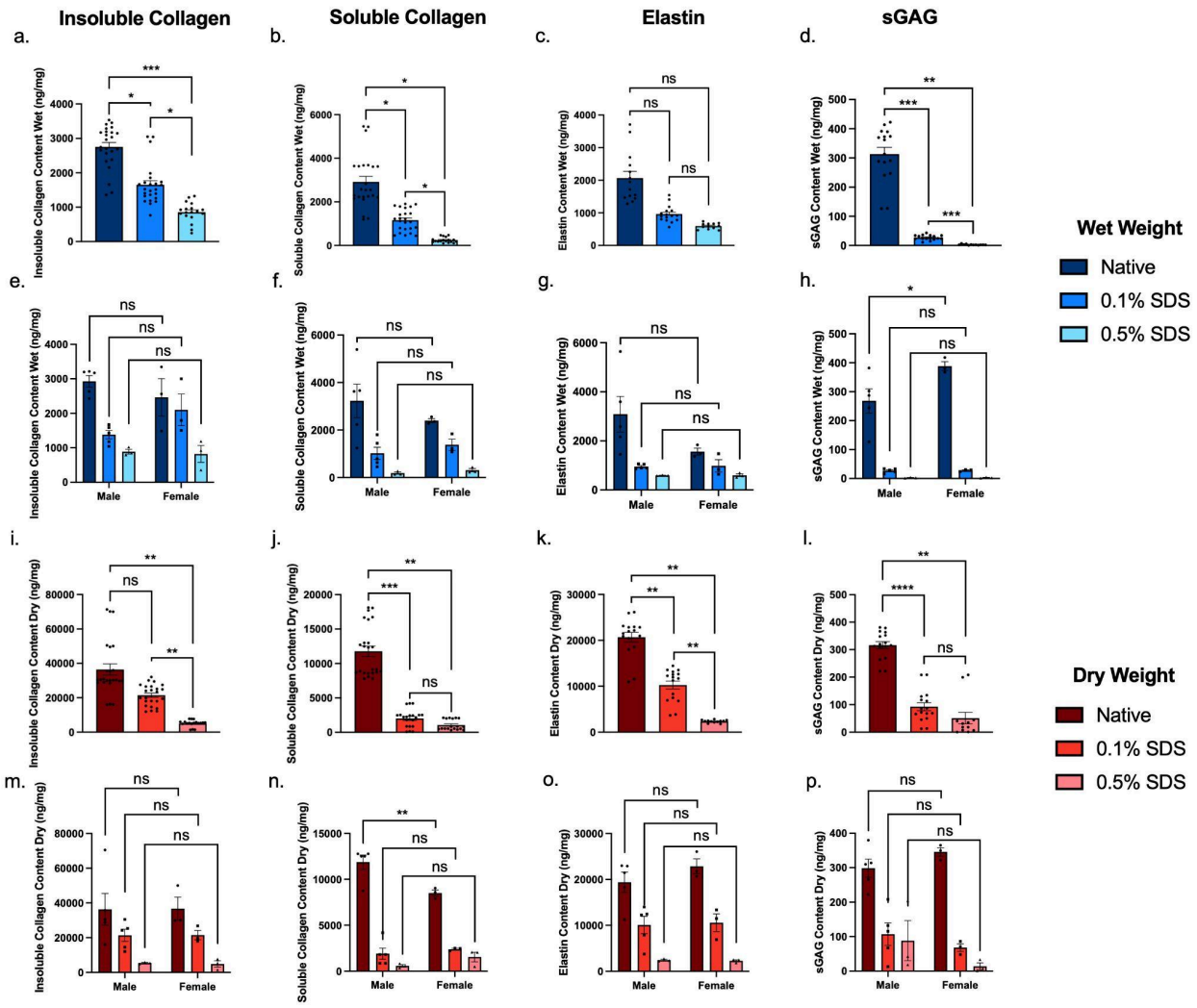


Figure 5. Quantitative analysis of extracellular matrix (ECM) protein content in human lung tissue. Wet- and dry-weight normalized measurements of major ECM components are shown without and with sex stratification. Panels (a–d) present non-stratified wet-weight data for insoluble collagen, soluble collagen, elastin, and sGAG, respectively. Panels (e–h) present the corresponding sex-stratified wet-weight data for male and female tissues. Panels (i–l) present non-stratified dry-weight data for insoluble collagen, soluble collagen, elastin, and sGAG, respectively. Panels (m–p) present the corresponding sex-stratified dry-weight data for male and female tissues. Data are expressed as mean ± SEM (n = 5 male, n = 3 female). Statistical significance is denoted as ****$p \leq 0.0001$, ***$p \leq 0.001$, **$p \leq 0.01$, and *$p \leq 0.05$.

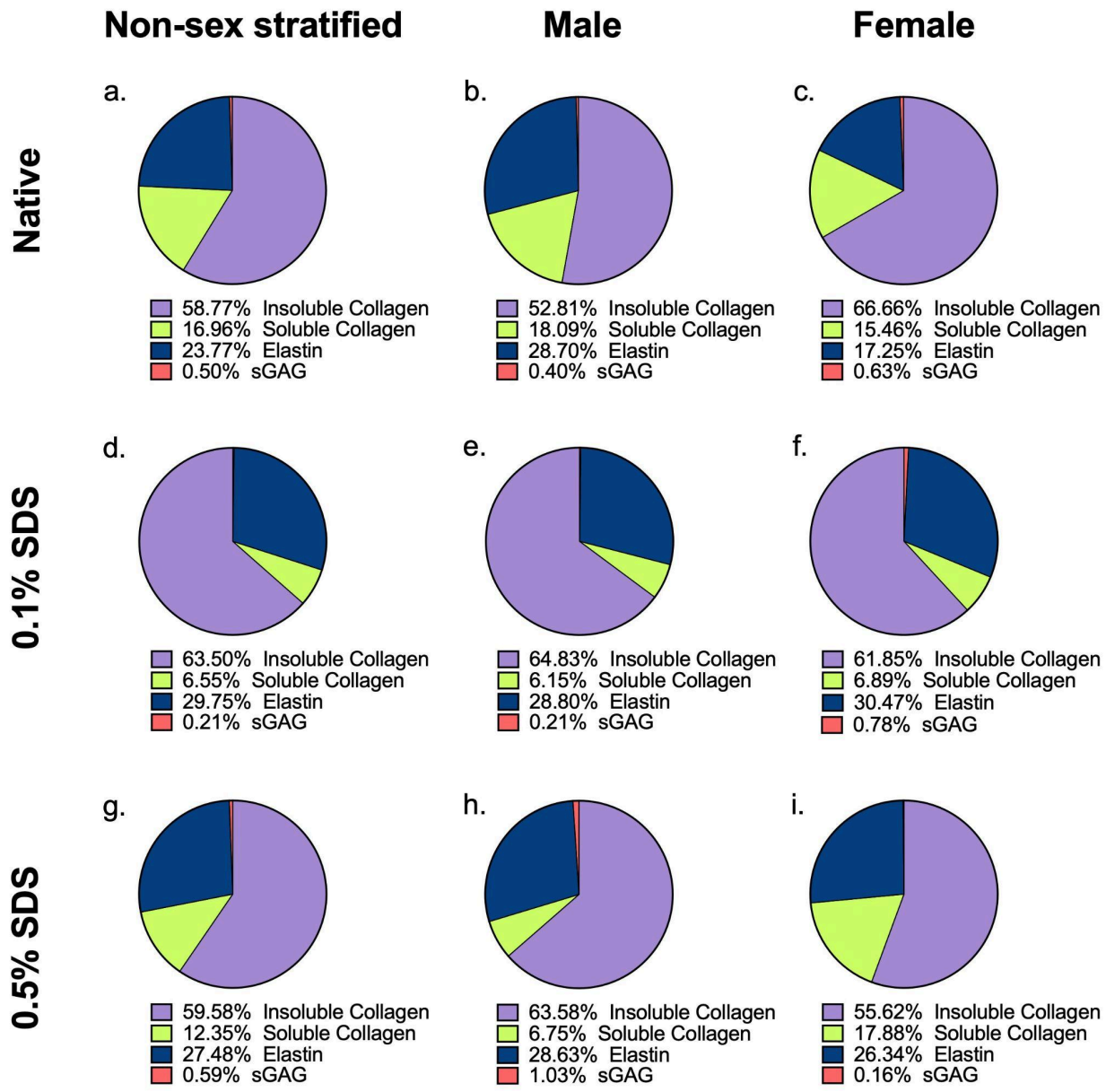


Figure 6. Relative extracellular matrix (ECM) composition of native and decellularized human lung tissue. Pie charts summarize the proportional contribution of insoluble collagen, soluble collagen, elastin, and sulfated glycosaminoglycans (sGAG) to the total measured ECM content in non-sex-stratified, male, and female groups for native tissue, 0.1% SDS dECM, and 0.5% SDS dECM. Values are calculated from mean ECM component abundances obtained from quantitative assays and are presented as percentages of the summed measured ECM content within each group. These charts provide a visual comparison of relative ECM composition and should be interpreted alongside the absolute quantitative data shown in Figure 5 and Table 4.

3.3.1 Insoluble Collagen

Insoluble collagen retention was significantly influenced by decellularization condition, with evidence of method-dependent differences in preserved matrix content following processing (Figure 5; Table 4). Under wet-weight normalization, mixed-effects analysis demonstrated a significant main effect of condition on insoluble collagen content ($p < 0.0001$) as well as a significant sex × condition interaction (p

= 0.0242), indicating that the effect of decellularization on retained insoluble collagen differed between male and female tissues. Post hoc comparisons of the overall condition means showed that native tissue contained significantly more insoluble collagen than both the 0.1% SDS group ($p = 0.0119$) and the 0.5% SDS group ($p = 0.0006$), while the 0.1% SDS group also retained significantly more insoluble collagen than the 0.5% SDS group ($p = 0.0314$).

Male native tissue contained 2929.07 ± 166.18 ng/mg insoluble collagen, which decreased to 1380.93 ± 119.75 ng/mg in the 0.1% SDS group and 887.78 ± 68.49 ng/mg in the 0.5% SDS group (Table 4). Female native tissue contained 2463.56 ± 540.09 ng/mg insoluble collagen, which decreased to 2100.00 ± 458.77 ng/mg following 0.1% SDS treatment and 822.00 ± 244.81 ng/mg following 0.5% SDS treatment (Table 4). These values corresponded to wet-weight retention of 47.15% and 30.31% in male tissues and 85.24% and 33.37% in female tissues for the 0.1% and 0.5% SDS groups, respectively. Within male tissues, native insoluble collagen content remained significantly higher than both the 0.1% SDS condition ($p = 0.0056$) and the 0.5% SDS condition ($p = 0.0019$), further supporting substantial method-dependent loss of insoluble collagen following decellularization.

A significant main effect of condition was also observed under dry-weight normalization ($p = 0.0066$), again supporting method-dependent differences in retained insoluble collagen content. Post hoc comparisons of the overall condition means showed that native tissue retained significantly more insoluble collagen than the 0.5% SDS group ($p = 0.0039$) and that the 0.1% SDS group also retained significantly more insoluble collagen than the 0.5% SDS group ($p = 0.0067$). Male native tissue contained 36328.00 ± 9136.07 ng/mg insoluble collagen, which decreased to 21340.67 ± 3474.41 ng/mg in the 0.1% SDS group and 5426.89 ± 293.53 ng/mg in the 0.5% SDS group (Table 4). Female native tissue contained 36691.33 ± 6656.19 ng/mg insoluble collagen, which decreased to 21467.78 ± 2704.12 ng/mg following 0.1% SDS treatment and 4809.11 ± 1814.18 ng/mg following 0.5% SDS treatment (Table 4). These corresponded to dry-weight retention values of 58.74% and 14.94% in male tissues and 58.51% and 13.11% in female tissues for the 0.1% and 0.5% SDS groups, respectively. Within female tissues, the 0.1% SDS group retained significantly more insoluble collagen than the 0.5% SDS group ($p = 0.0199$). Together, these findings show that insoluble collagen preservation was strongly dependent on decellularization method, with the 0.1% SDS protocol retaining more insoluble collagen than the 0.5% SDS protocol.

3.3.2 Soluble Collagen

Soluble collagen retention was significantly influenced by decellularization condition under both wet- and dry-weight normalization, with additional sex-dependent effects observed under dry-weight normalization (Figure 5; Table 4). Under wet-weight normalization, mixed-effects analysis demonstrated a significant main effect of condition on soluble collagen content ($p = 0.0022$). Post hoc comparisons of the overall condition means showed that native tissue contained significantly more soluble collagen than both the 0.1% SDS group ($p = 0.0421$) and the 0.5% SDS group ($p = 0.0196$), while the 0.1% SDS group also retained significantly more soluble collagen than the 0.5% SDS group ($p = 0.0341$).

Male native tissue contained 3232.11 ± 705.22 ng/mg soluble collagen, which decreased to 1023.02 ± 256.41 ng/mg in the 0.1% SDS group and 183.42 ± 44.84 ng/mg in the 0.5% SDS group (Table 4). Female native tissue contained 2398.66 ± 83.18 ng/mg soluble collagen, which decreased to 1382.81 ±

233.97 ng/mg following 0.1% SDS treatment and 307.61 ± 68.90 ng/mg following 0.5% SDS treatment (Table 4). These values corresponded to wet-weight retention of 31.65% and 5.67% in male tissues and 57.65% and 12.82% in female tissues for the 0.1% and 0.5% SDS groups, respectively. Within female tissues, native soluble collagen content remained significantly higher than the 0.5% SDS condition ($p = 0.0104$), further supporting reduced retention of soluble collagen following the higher detergent treatment.

Under dry-weight normalization, mixed-effects analysis again demonstrated a significant main effect of condition ($p < 0.0001$) as well as a significant sex × condition interaction ($p = 0.0198$), indicating that the effect of decellularization on retained soluble collagen differed between male and female tissues. Post hoc comparisons of the overall condition means showed that native tissue contained significantly more soluble collagen than both the 0.1% SDS group ($p = 0.0003$) and the 0.5% SDS group ($p = 0.0016$). Male native tissue contained 13727.68 ± 1636.38 ng/mg soluble collagen, which decreased to 1736.85 ± 887.20 ng/mg in the 0.1% SDS group and 575.90 ± 138.69 ng/mg in the 0.5% SDS group (Table 4). Female native tissue contained 8509.53 ± 334.99 ng/mg soluble collagen, which decreased to 2392.65 ± 95.39 ng/mg following 0.1% SDS treatment and 1545.90 ± 516.51 ng/mg following 0.5% SDS treatment (Table 4). These corresponded to dry-weight retention values of 12.65% and 4.20% in male tissues and 28.12% and 18.17% in female tissues for the 0.1% and 0.5% SDS groups, respectively. Within male tissues, native soluble collagen content remained significantly higher than the 0.1% SDS condition ($p = 0.0055$). Within female tissues, native soluble collagen content remained significantly higher than both the 0.1% SDS ($p = 0.0133$) and 0.5% SDS ($p = 0.0388$) conditions. In addition, native male tissue contained significantly more soluble collagen than native female tissue ($p = 0.0098$). Together, these findings show that soluble collagen preservation was strongly influenced by decellularization method, with additional sex-dependent differences becoming more apparent under dry-weight normalization.

3.3.3 Elastin

Elastin retention was influenced by decellularization condition, with condition-dependent differences observed in preserved matrix content following processing (Figure 5; Table 4). Under wet-weight normalization, mixed-effects analysis demonstrated a significant main effect of condition on elastin content ($p = 0.0270$), indicating that elastin levels varied across native and decellularized tissues. Male native tissue contained 3085.90 ± 726.81 ng/mg elastin, which decreased to 952.60 ± 42.62 ng/mg in the 0.1% SDS group and 592.83 ± 5.55 ng/mg in the 0.5% SDS group (Table 4). Female native tissue contained 1563.17 ± 139.54 ng/mg elastin, which decreased to 981.50 ± 253.33 ng/mg following 0.1% SDS treatment and 597.67 ± 53.36 ng/mg following 0.5% SDS treatment (Table 4). These values corresponded to wet-weight retention of 30.87% and 19.21% in male tissues and 62.79% and 38.23% in female tissues for the 0.1% and 0.5% SDS groups, respectively. Together, these findings indicate that elastin retention was altered following decellularization under wet-weight normalization.

A stronger condition-dependent effect was observed under dry-weight normalization. Mixed-effects analysis demonstrated a significant main effect of condition on elastin content ($p < 0.0001$). Post hoc comparisons of the overall condition means showed that native tissue contained significantly more elastin than both the 0.1% SDS group ($p = 0.0041$) and the 0.5% SDS group ($p = 0.0012$), while the 0.1% SDS group also retained significantly more elastin than the 0.5% SDS group ($p = 0.0030$). Male native tissue contained 19390.60 ± 2200.76 ng/mg elastin, which decreased to 10076.70 ± 1879.20 ng/mg in the 0.1% SDS group and 2443.80 ± 157.57 ng/mg in the 0.5% SDS group (Table 4). Female native tissue contained

22866.33 ± 1633.56 ng/mg elastin, which decreased to 10575.50 ± 1927.15 ng/mg following 0.1% SDS treatment and 2276.85 ± 223.07 ng/mg following 0.5% SDS treatment (Table 4). These corresponded to dry-weight retention values of 51.97% and 12.60% in male tissues and 46.25% and 9.96% in female tissues for the 0.1% and 0.5% SDS groups, respectively. Within female tissues, native elastin content remained significantly higher than the 0.5% SDS condition ($p = 0.0159$). Overall, these findings show that elastin preservation was reduced following decellularization and that the 0.1% SDS protocol retained more elastin than the 0.5% SDS protocol under dry-weight normalization.

3.3.4 sGAG

sGAG content was strongly influenced by decellularization condition, demonstrating substantial loss of this matrix-associated component following processing (Figure 5; Table 4). Under wet-weight normalization, mixed-effects analysis demonstrated a significant main effect of condition on sGAG content ($p = 0.0001$). Post hoc comparisons of the overall condition means showed that native tissue contained significantly more sGAG than both the 0.1% SDS group ($p = 0.0002$) and the 0.5% SDS group ($p = 0.0028$), while the 0.1% SDS group also retained significantly more sGAG than the 0.5% SDS group ($p = 0.0003$).

Male native tissue contained 268.40 ± 41.83 ng/mg sGAG, which decreased to 26.93 ± 3.34 ng/mg in the 0.1% SDS group and 2.17 ± 0.82 ng/mg in the 0.5% SDS group (Table 4). Female native tissue contained 388.64 ± 15.15 ng/mg sGAG, which decreased to 27.76 ± 2.01 ng/mg following 0.1% SDS treatment and 2.51 ± 0.88 ng/mg following 0.5% SDS treatment (Table 4). These values corresponded to wet-weight retention of 10.03% and 0.81% in male tissues and 7.14% and 0.64% in female tissues for the 0.1% and 0.5% SDS groups, respectively. Within male tissues, native sGAG content remained significantly higher than the 0.1% SDS condition ($p = 0.0116$). Within female tissues, native sGAG content remained significantly higher than both the 0.1% SDS ($p = 0.0051$) and 0.5% SDS ($p = 0.0051$) conditions, and the 0.1% SDS group also retained significantly more sGAG than the 0.5% SDS group ($p = 0.0184$). In addition, native female tissue contained significantly more sGAG than native male tissue ($p = 0.0431$), indicating a baseline sex-dependent difference in wet-weight normalized sGAG content.

Under dry-weight normalization, mixed-effects analysis again demonstrated a significant main effect of condition ($p = 0.0002$). Post hoc comparisons of the overall condition means showed that native tissue contained significantly more sGAG than both the 0.1% SDS group ($p < 0.0001$) and the 0.5% SDS group ($p = 0.0018$). Male native tissue contained 298.39 ± 26.34 ng/mg sGAG, which decreased to 107.21 ± 32.68 ng/mg in the 0.1% SDS group and 88.32 ± 58.16 ng/mg in the 0.5% SDS group (Table 4). Female native tissue contained 345.78 ± 12.54 ng/mg sGAG, which decreased to 68.17 ± 11.06 ng/mg following 0.1% SDS treatment and 13.80 ± 9.92 ng/mg following 0.5% SDS treatment (Table 4). These corresponded to dry-weight retention values of 35.93% and 29.60% in male tissues and 19.72% and 3.99% in female tissues for the 0.1% and 0.5% SDS groups, respectively. Within male tissues, native sGAG content remained significantly higher than the 0.1% SDS condition ($p = 0.0036$). Within female tissues, native sGAG content remained significantly higher than both the 0.1% SDS ($p = 0.0209$) and 0.5% SDS ($p = 0.0046$) conditions. Together, these findings show that sGAG content was substantially reduced following decellularization, with strong evidence of condition-dependent loss under both normalization approaches.

3.4 Cell Viability

Cell viability following exposure to human dECM was assessed using Live/Dead fluorescence staining of NIH 3T3 fibroblasts cultured in dECM-conditioned media and by Alamar Blue analysis of cells cultured directly on dECM tissue (Figure 7). Representative fluorescence images showed predominantly live, calcein AM-positive cells across all groups over the 3-day culture period, with minimal propidium iodide signal observed in the conditioned-media experiments (Figure 7A). Quantitative image analysis further demonstrated high overall viability in all groups (Figure 7B). On Day 1, average cell viability was 98.83 ± 0.46% in the control group, 98.73 ± 0.50% in the male dECM-conditioned media group, and 98.56 ± 0.20% in the female dECM-conditioned media group. By Day 2, viability remained high at 96.31 ± 1.02% in controls, 94.15 ± 2.33% in the male dECM group, and 94.43 ± 0.44% in the female dECM group. On Day 3, viability was 96.69 ± 0.75% in controls, 91.63 ± 4.32% in the male dECM group, and 90.77 ± 0.74% in the female dECM group. Collectively, these data indicate that conditioned media derived from human dECM supported high cell viability over the duration of the assay.

Direct-contact imaging also showed that 3T3 cells remained present on both male and female human dECM tissues following a 3 day culture, with predominantly live-cell fluorescence observed in both groups (Figure 7C). Metabolic activity assessed by Alamar Blue revealed variability between donor groups and across time points, but measurable cell activity was maintained throughout the 3-day culture period (Figure 7D). In male dECM groups, normalized viability values were 91.45 ± 5.57% on Day 1, 62.68 ± 16.79% on Day 2, and 82.80 ± 19.09% on Day 3. In female dECM groups, normalized viability values were 98.56 ± 8.95% on Day 1, 105.90 ± 17.26% on Day 2, and 122.52 ± 14.98% on Day 3. Together, the Live/Dead and Alamar Blue results support the ability of human dECM to maintain viable cells in both conditioned-media and direct-contact culture settings.

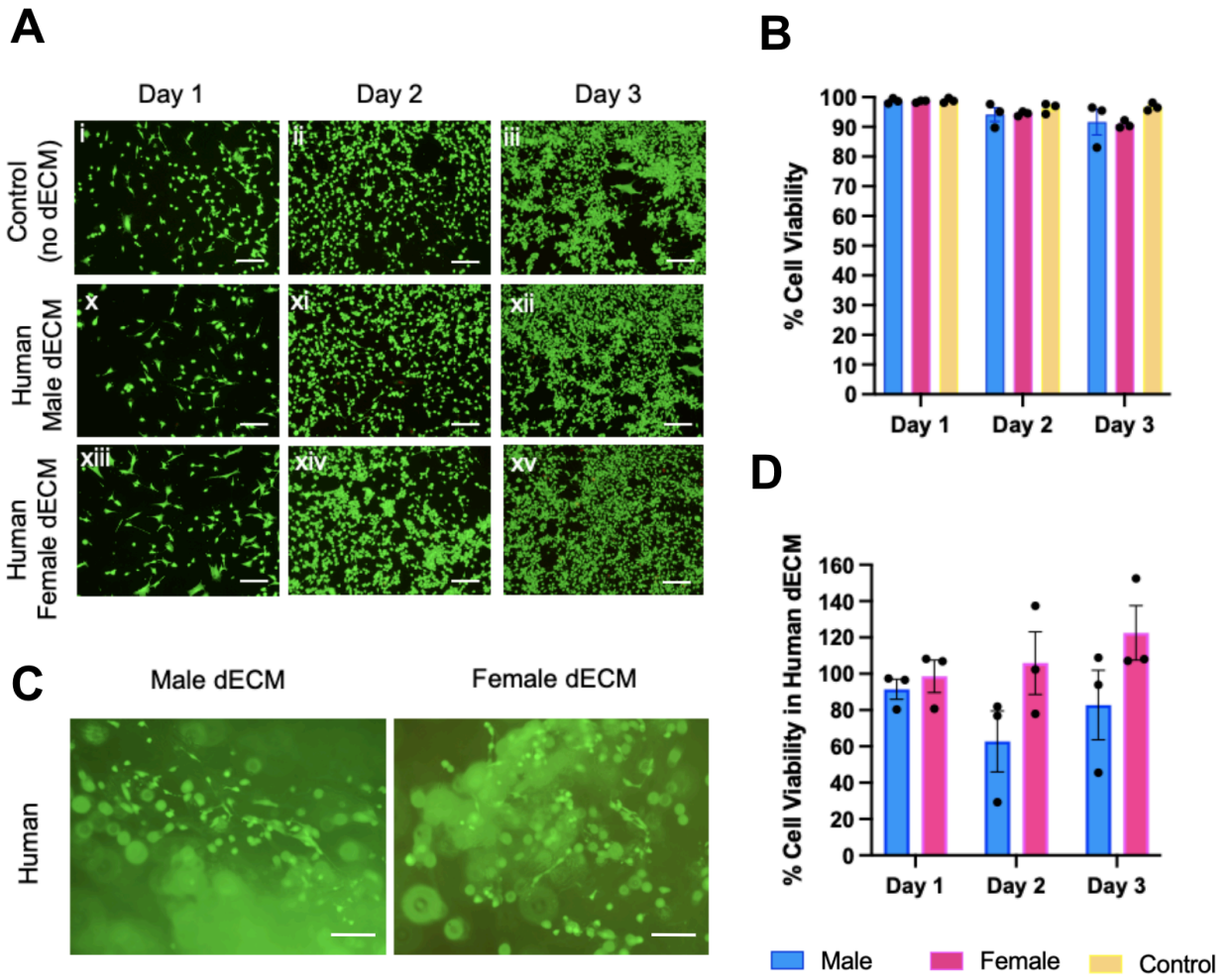


Figure 7. Assessment of cell viability following exposure to dECM. (A) Representative live/dead fluorescence images of 3T3 cells cultured with dECM conditioned media for 3 days. Live cells are stained with calcein AM (green), and dead cells with propidium iodide (red). Scale bar = 100 µm. (B) Quantitative analysis of cell viability derived from image processing (MATLAB) on human dECM. (C) 3T3 cells on the dECM tissue that were cultured for 3 days. Live cells are stained with calcein AM (green), and dead cells with propidium iodide (red). Scale bar = 100 µm. (D) Metabolic activity assessed using the Alamar Blue assay following 3 days of direct dECM contact.

3.5 Idiopathic Pulmonary Fibrosis

Preliminary biochemical characterization was also performed on one male and one female IPF human lung donor to provide an exploratory comparison of diseased tissue before and after decellularization using the 0.1% SDS protocol (Figure 8; Table 5). Both wet- and dry-weight normalized values are shown for all assays. Because these data represent n = 1 male IPF donor and n = 1 female IPF donor, values are presented as mean ± SD of technical replicates, and statistical comparisons between native and decellularized IPF tissues were performed using unpaired parametric t-tests with Welch's correction. These analyses are intended for exploratory comparison only and should not be interpreted as definitive

biological conclusions, but rather as a preliminary assessment of how ECM composition in IPF lung tissue changes following decellularization.

DNA content decreased substantially after decellularization in both IPF samples under both normalization approaches. Under wet-weight normalization, DNA content decreased from 250.67 ± 8.02 ng/mg to 20.33 ± 7.57 ng/mg in the male donor and from 549.33 ± 13.01 ng/mg to 40.00 ± 3.00 ng/mg in the female donor, corresponding to reductions of 91.89% and 92.72%, respectively. Under dry-weight normalization, DNA content decreased from 861.50 ± 58.59 ng/mg to 16.17 ± 2.08 ng/mg in the male donor and from 738.50 ± 19.05 ng/mg to 55.83 ± 1.53 ng/mg in the female donor, corresponding to reductions of 98.12% and 92.44%, respectively. Total protein content also decreased after decellularization. Under wet-weight normalization, male total protein content decreased from 10022.59 ± 555.73 ng/mg to 1122.68 ± 26.50 ng/mg, while female total protein content decreased from 13752.45 ± 162.72 ng/mg to 1439.59 ± 70.95 ng/mg. Under dry-weight normalization, male total protein decreased from 10420.07 ± 158.42 ng/mg to 5289.00 ± 4214.85 ng/mg, whereas female total protein decreased from 10447.39 ± 64.43 ng/mg to 1010.79 ± 41.17 ng/mg.

ECM-specific assays further suggested sex-dependent differences in matrix composition before and after decellularization. For insoluble collagen, the male native IPF sample showed substantially higher dry-weight content (69021.33 ± 837.63 ng/mg) than the female native sample (13170.67 ± 232.18 ng/mg), whereas the female dECM sample retained markedly more insoluble collagen (12986.00 ± 192.32 ng/mg) than the male dECM sample (2748.67 ± 113.50 ng/mg). Soluble collagen was also higher in the male native sample under both wet- and dry-weight normalization, but the female sample retained a greater proportion of soluble collagen after decellularization. Elastin content decreased after decellularization in both donors, with native male tissue showing higher elastin content than native female tissue under both normalization methods. For sGAG, wet-weight values were low after decellularization in both donors, whereas dry-weight values suggested greater retention in the male sample (257.21 ± 2.88 ng/mg) than in the female sample (201.20 ± 4.34 ng/mg). Together, these preliminary observations suggest that disease-state and sex-dependent differences in ECM composition may persist in both native and decellularized IPF lung tissue and support future expansion of diseased donor analysis.

Table 5. Preliminary biochemical characterization of IPF human lung tissue normalized to wet and dry weight. Values are presented as mean ± standard deviation (SD) from technical replicates for n = 1 male IPF donor and n = 1 female IPF donor processed using the 0.1% SDS decellularization protocol.

Parameter of Interest	Normalization	Sex	Native (ng/mg)	0.1% SDS dECM (ng/mg)	% Reduction or % Retention (0.1% SDS)
DNA	Wet weight	Male	250.67 ± 8.02	20.33 ± 7.57	91.89% reduction
	Wet weight	Female	549.33 ± 13.01	40.00 ± 3.00	92.72% reduction
	Dry weight	Male	861.50 ± 58.59	16.17 ± 2.08	98.12% reduction
	Dry weight	Female	738.50 ± 19.05	55.83 ± 1.53	92.44% reduction
Total Protein	Wet weight	Male	10022.59 ± 555.73	1122.68 ± 26.50	11.20% retention
	Wet weight	Female	13752.45 ± 162.72	1439.59 ± 70.95	10.47% retention
	Dry weight	Male	10420.07 ± 158.42	5289.00 ± 4214.85	50.76% retention
	Dry weight	Female	10447.39 ± 64.43	1010.79 ± 41.17	9.68% retention
Insoluble Collagen	Wet weight	Male	5124.00 ± 118.03	872.00 ± 109.56	17.02% retention
	Wet weight	Female	1316.67 ± 37.81	815.33 ± 104.43	61.92% retention
	Dry weight	Male	69021.33 ± 837.63	2748.67 ± 113.50	3.98% retention
	Dry weight	Female	13170.67 ± 232.18	12986.00 ± 192.32	98.60% retention
Soluble Collagen	Wet weight	Male	4824.21 ± 38.16	1771.23 ± 13.99	36.72% retention
	Wet weight	Female	1346.14 ± 549.10	702.63 ± 23.99	52.20% retention
	Dry weight	Male	18318.25 ± 30.63	2070.53 ± 93.99	11.30% retention
	Dry weight	Female	4780.88 ± 57.10	2884.56 ± 67.25	60.34% retention
Elastin	Wet weight	Male	6427.50 ± 433.46	1475.50 ± 231.22	22.96% retention
	Wet weight	Female	3142.00 ± 62.23	1562.50 ± 75.66	49.73% retention
	Dry weight	Male	27187.00 ± 429.92	11784.00 ± 722.66	43.34% retention
	Dry weight	Female	20888.50 ± 655.49	6353.50 ± 153.44	30.42% retention
sGAG	Wet weight	Male	177.58 ± 0.15	26.57 ± 1.65	14.96% retention
	Wet weight	Female	164.84 ± 1.13	25.35 ± 0.66	15.38% retention
	Dry weight	Male	284.72 ± 4.13	257.21 ± 2.88	90.34% retention
	Dry weight	Female	342.22 ± 5.00	201.20 ± 4.34	58.79% retention

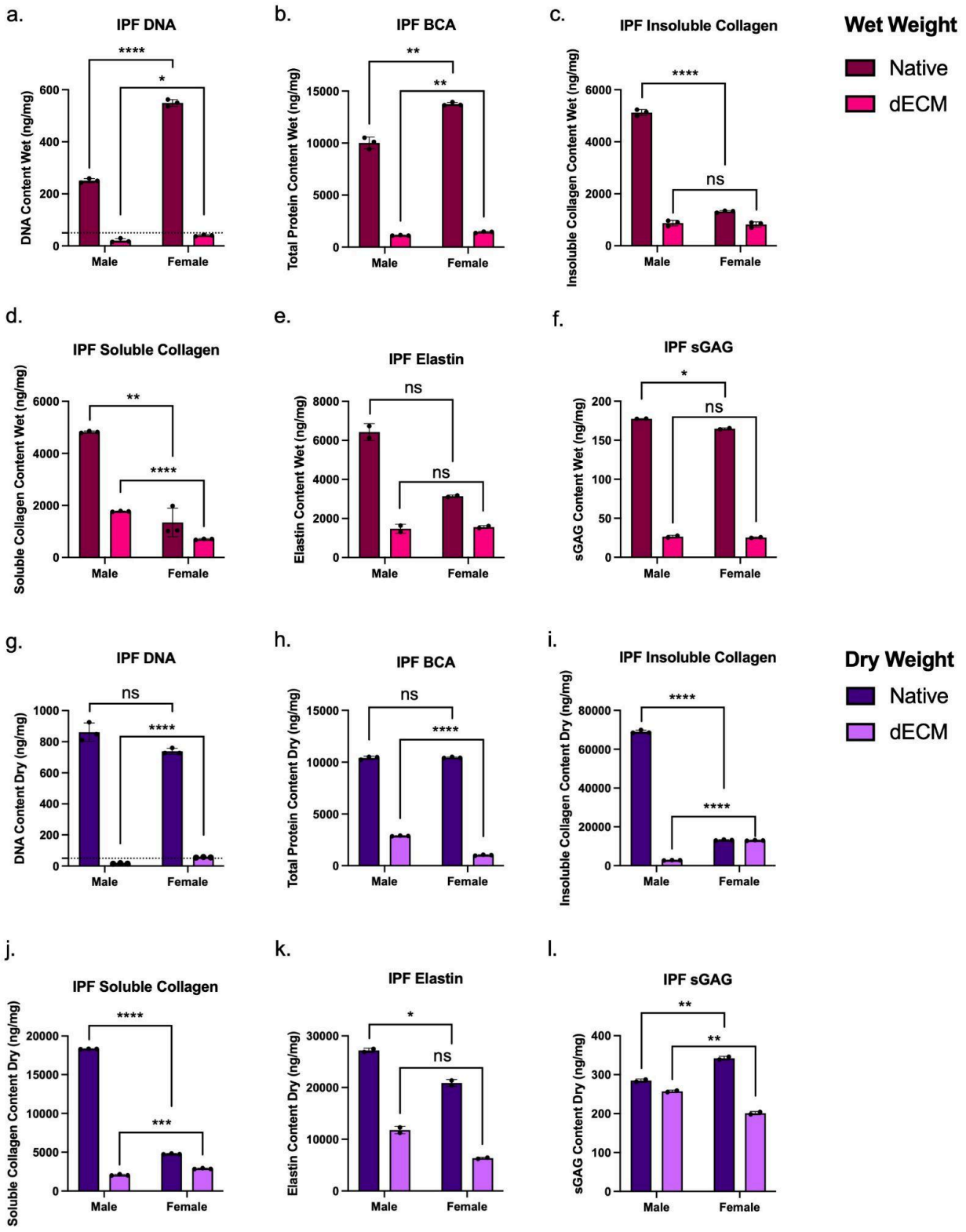


Figure 8. Preliminary biochemical characterization of native and decellularized idiopathic pulmonary fibrosis (IPF) human lung tissue. Wet- and dry-weight normalized content values are shown for native and decellularized extracellular matrix (dECM) IPF lung tissues processed using the 0.1% SDS protocol. Panels (a–f) present

wet-weight data for DNA, total protein, insoluble collagen, soluble collagen, elastin, and sulfated glycosaminoglycan (sGAG), respectively. Panels (g–l) present the corresponding dry-weight data for DNA, total protein, insoluble collagen, soluble collagen, elastin, and sGAG, respectively. Native tissues are shown in the darker color and dECM tissues in the lighter color for each normalization condition. Data are presented as preliminary observations from n = 1 male IPF donor and n = 1 female IPF donor with technical replicates and are included for exploratory comparison with healthy tissue datasets. Data are expressed as mean ± SD of technical replicates. Statistical significance is denoted as ****$p \leq 0.0001$, ***$p \leq 0.001$, **$p \leq 0.01$, and *$p \leq 0.05$.

4. Discussion

In this study, both human lung decellularization protocols achieved the major hallmarks of effective cell removal [10], but they did not produce compositionally equivalent scaffolds. As shown in Figure 3A–C and Table 2, both the 0.1% SDS and 0.5% SDS conditions markedly reduced residual DNA, eliminated visible nuclear staining, and diminished DNA banding relative to native tissue, supporting successful decellularization by standard qualitative and quantitative criteria. However, once the analysis moved beyond DNA removal and into retained matrix composition as seen in Figures 4-5 and Tables 3-4, clear differences emerged between the two protocols. Overall, the 0.1% SDS condition significantly preserved more total protein and more of several key extracellular matrix components than the 0.5% SDS condition, particularly for insoluble collagen, soluble collagen, elastin, and sGAG. Sex-based differences were present, but they were selective rather than global, appearing only in specific components and under specific wet and dry normalization or processing conditions rather than as a uniform male-versus-female shift across the entire matrix. Importantly, both human dECM groups also supported short-term fibroblast viability, indicating that the resulting materials were not only effectively decellularized, but also remained usable as biomaterial platforms for downstream cell studies.

These findings fit well with the broader lung decellularization literature, which shows that dECM quality cannot be judged by DNA removal alone [26]. Commonly used decellularization benchmarks emphasize low residual DNA content, short DNA fragment length, and absence of visible nuclei, but those criteria do not capture how strongly a protocol alters the retained biochemical environment [10], [27]. Although both methods met the major decellularization criteria in Figure 3, the 0.1% SDS condition retained significantly more insoluble collagen than 0.5% SDS under both wet- and dry-weight normalization (Figure 5; Table 4), significantly more soluble collagen under wet-weight normalization, significantly more elastin under dry-weight normalization, and significantly more sGAG under wet-weight normalization. By contrast, total protein in Figure 4 was significantly reduced in both decellularized groups relative to native tissue, but the difference between 0.1% SDS and 0.5% SDS was not consistently significant, suggesting that bulk protein loss alone does not fully capture the more selective matrix effects seen in the ECM-specific assays. That distinction is especially important in lung tissue, where previous comparative studies have shown that the choice of detergent and concentration changes matrix retention patterns in meaningful ways [15]. O'Neill and colleagues reported that a low concentration CHAPS-decellularized lung tissue showed the best retention of lung ECM structure compared with other detergent approaches, supporting the idea that harsher ionic processing can come at the expense of matrix preservation. Likewise, Wagner et al. showed that decellularized human lungs could retain overall architecture and collagen while still losing important matrix constituents such as elastin and glycosaminoglycans [28]. Mechanistically, that interpretation is also supported by broader decellularization literature showing that SDS, as an ionic detergent, is highly effective for membrane and

nuclear removal but can also denature proteins, disrupt basement-membrane-associated components, and deplete sulfated glycosaminoglycans during repeated exposure and washing [15], [16], [17]. In that context, the greater matrix loss seen with 0.5% SDS in this study is biologically plausible since increasing detergent strength likely improved solubilization of cellular material, but at the cost of extracting or destabilizing ECM components that are more detergent-sensitive, particularly sGAGs, soluble collagen fractions, and elastin-associated structure [29]. Uhl et al. further showed that lung GAG depletion after decellularization is not merely quantitative, but can also impair matrix function, reinforcing why the strong sGAG losses in Figure 5 may matter beyond simple composition alone [30].

A second important finding of the present study is that sex-based differences were present, but they were selective rather than global, and in several cases were only detectable within particular matrix proteins or normalization strategies (wet weight vs. dry weight). Across Figures 4–5, sex was not the dominant source of variation; however, direct male-versus-female differences were still identified in specific native ECM measures. Most notably, native male tissue contained significantly more dry-weight soluble collagen than native female tissue, whereas native female tissue contained significantly more wet-weight sGAG than native male tissue (Figure 5; Table 4). In addition, significant sex × condition interactions were detected for wet-weight insoluble collagen and dry-weight soluble collagen, indicating that the effect of decellularization on those ECM components differed between male and female tissues even when direct pairwise sex comparisons were not uniformly significant after correction. Together, these results suggest that sex-related biological differences exist within the native lung matrix, but that their detectability after decellularization is partly shaped by processing methods. This interpretation of the need for considering sex-based differences is consistent with the broader literature. The recent American Thoracic Society research statement on sex as a biological variable in lung research emphasizes that pulmonary phenotypes are influenced by sex across the lifespan and that preclinical lung models should explicitly account for sex rather than treat it as a background descriptor [20]. In idiopathic pulmonary fibrosis (IPF), McGee et al. reported sex-associated differences in fibrosis-related gene expression, including MMP7 and CHI3L1, and clinical cohort studies continue to show that IPF is male-dominant and associated with poorer outcomes in men [25], [31]. Outside the lung, Simon et al. showed that male valvular interstitial cells exhibited greater myofibroblastic activation and collagen production, whereas female cells showed higher matrix metalloproteinase activity and metabolic activity [21], and Sarver et al. reported that female mouse tendon exhibited modestly greater ECM protein and proteoglycan content despite similar overall mechanical behavior [22]. Collectively, these studies support the idea that sex-related ECM differences are biologically plausible, but are often component-specific and context-dependent rather than uniformly detectable across every matrix readout.

These method-dependent differences are not just biochemical readouts, because retained collagen, elastin, and sGAGs help define both the mechanical and biochemical environment that cells experience within the scaffold. In lung parenchyma, collagen is a major load-bearing ECM component that contributes to tensile stiffness and force transmission [32], whereas elastin supports reversible stretch and recoil during breathing [33], therefore shifting the balance between these components can therefore change how strain is distributed through the matrix and how cells mechanically experience their surroundings [34]. The distinction between insoluble and soluble collagen is also important in this context. Insoluble collagen more closely reflects the mature, cross-linked fibrillar collagen network that stabilizes tissue architecture and resists deformation, whereas soluble collagen represents a more extractable collagen pool that is likely more vulnerable to processing-related loss [35]. Studies investigating collagen and elastin

cross-linking have shown that these cross-linked matrix networks are closely tied to tissue stability, remodeling, and mechanical behavior, including during lung development and injury [34], [36]. sGAGs contribute differently but just as importantly, because they regulate hydration, matrix viscoelasticity, and growth factor presentation within the ECM [30]. Uhl et al. showed that depletion of glycosaminoglycans from decellularized lung ECM reduced FGF2 and VEGF binding and altered downstream cellular responses, demonstrating that sGAG loss changes scaffold function as well as scaffold composition. This is particularly relevant to the present study because the 0.1% SDS condition retained significantly more insoluble collagen than 0.5% SDS under both wet- and dry-weight normalization, significantly more soluble collagen under wet-weight normalization, significantly more elastin under dry-weight normalization, and significantly more sGAG under wet-weight normalization (Figure 5; Table 4). However, the relative ECM composition profiles shown in Figure 6 add an important layer of interpretation. In the non-sex-stratified comparison, native tissue consisted of 58.77% insoluble collagen, 16.96% soluble collagen, 23.77% elastin, and 0.50% sGAG, whereas the 0.1% SDS group shifted to 63.50% insoluble collagen, 6.55% soluble collagen, 29.75% elastin, and 0.21% sGAG, while the 0.5% SDS group measured 59.58% insoluble collagen, 12.35% soluble collagen, 27.48% elastin, and 0.59% sGAG. Similar patterns were observed in the male and female stratified charts, where the 0.5% SDS group showed a proportional ECM profile that was slightly closer to native than the 0.1% SDS group, particularly in the non-sex-stratified and female comparisons. For example, in the female samples, native tissue was composed of 66.66% insoluble collagen, 15.46% soluble collagen, 17.25% elastin, and 0.63% sGAG, compared with 61.85%, 6.89%, 30.47%, and 0.78% in the 0.1% SDS group and 55.62%, 17.88%, 26.34%, and 0.16% in the 0.5% SDS group, indicating that although both methods altered the matrix, the 0.5% SDS condition more closely approximated the native relative distribution of several ECM components. Importantly, these pie charts reflect proportional composition only, not absolute retention. Thus, when Figure 6 is interpreted together with the quantitative data in Figure 5 and Table 4, the overall picture is that 0.1% SDS preserved greater absolute amounts of several key ECM components, whereas 0.5% SDS in some cases retained a relative ECM balance that appeared closer to native because of more globally distributed matrix loss. Functionally, this suggests that the two decellularization methods do not simply preserve more or less matrix overall, but instead reshape the retained biochemical environment in different ways, which may influence the fibrillar tensile framework, elastic recoil potential, viscoelasticity, and biochemical signaling reservoir presented to cells. That interpretation is consistent with studies showing that human lung dECM hydrogels can reproduce native-like stiffness and viscoelasticity and can support 2D and 3D lung cell culture, meaning that differences in retained ECM fractions are likely to translate into different cues delivered to cells in future hydrogel, bioink, and mechanotransduction applications [37], [38].

These compositional differences matter because cells do not respond to isolated matrix proteins one at a time, but rather they integrate stiffness, viscoelasticity, ligand availability, and growth factor presentation simultaneously through mechanotransductive pathways [8]. When that surrounding microenvironment is oversimplified, such as on rigid tissue culture plastic or in single-component matrices, cellular behaviors including spreading, contraction, migration, matrix deposition, and profibrotic activation may no longer reflect what occurs in native lung tissue [39]. Studies using human lung dECM hydrogels have shown that these materials can reproduce native-like stiffness and viscoelasticity, while decellularized human lung bioinks have also been shown to support 2D and 3D lung cell culture, highlighting why tissue-representative platforms are needed for biologically relevant lung models [37], [38]. Booth et al.

further showed that fibroblasts cultured on normal versus fibrotic human lung matrices underwent distinct molecular responses, demonstrating that the matrix itself can drive downstream cell behavior in a disease-relevant manner [40]. In that context, preserving a representative lung microenvironment is not just advantageous for biomaterial design, it is necessary for studying mechanotransduction in a way that more physiologically reflects how lung cells interpret ECM composition and mechanics in vivo [40]. The present findings therefore support the 0.1% SDS condition as the better starting point for future human lung dECM hydrogels, cell-seeded scaffolds, and mechanobiology studies, because a scaffold that better retains collagen fractions, elastin, and sGAG is more likely to preserve the native cues that regulate downstream cellular function.

In addition to preserving key ECM fractions, the resulting human dECM remained cytocompatible, which is important not only for short-term viability but also as an early indicator that the scaffold may be suitable for future recellularization. In Figure 7, conditioned media generated from decellularized human lung tissue did not produce overt cytotoxicity, and fibroblasts remained viable in both the conditioned-media and direct-contact studies over the culture period. Importantly, the direct-contact live/dead imaging on dECM over 3 days also showed that fibroblasts were not simply surviving on the surface, but were able to associate with and integrate into the 3D scaffold, supporting the idea that the material can function as a cell-permissive matrix rather than only as an inert substrate. These findings suggest that residual processing reagents were removed sufficiently to permit early cell survival and cell–matrix interaction, which is a necessary first step for successful reseeding [28]. That interpretation is consistent with Booth et al., who showed that normal human fibroblasts could be reseeded into acellular normal and IPF human lung matrix slices, migrate into the 3D matrix, and then be analyzed for downstream phenotypic responses [40]. It is also consistent with studies showing that processed human lung dECM can function as a true cell-facing biomaterial in multiple formats such as in the study by de Hilster et al. that demonstrated that human lung dECM hydrogels retain native-like stiffness and viscoelasticity, and Dabaghi et al. showed that decellularized human lung bioinks are amenable to 2D and 3D lung cell culture [37], [38]. Taken together, the viability data in the present study support not only short-term cytocompatibility, but also the broader conclusion that these matrices can be further developed into recellularizable human lung platforms for future studies of fibroblast behavior, matrix remodeling, regeneration, and mechanotransduction.

Although the IPF dataset in the present study was exploratory, it is still important because IPF is fundamentally a disease of abnormal ECM accumulation and remodeling, and those matrix changes are closely tied to altered tissue mechanics [41]. In IPF, excessive deposition of fibrillar collagens and other matrix-associated components, together with changes in elastin organization and matrix composition, produces a lung microenvironment that is mechanically distinct from healthy tissue and substantially stiffer than normal lung [42]. Booth et al. showed that acellular IPF human lung matrices were enriched in glycosaminoglycans, periostin, latent TGF-β binding protein 1, and collagens including collagen I, collagen III, and collagen VI, and that acellular IPF matrices were markedly stiffer than normal acellular lung matrices, with a mean Young's modulus of approximately 7.34 kPa compared with approximately 1.60 kPa in normal lung matrix [40]. In the same study, normal human fibroblasts cultured within IPF matrix showed increased α-smooth muscle actin (α-SMA) expression compared with fibroblasts cultured in normal matrix, consistent with myofibroblast differentiation, demonstrating that the altered fibrotic matrix itself can drive downstream cellular behavior. This concept is further supported by studies showing that increasing matrix stiffness promotes fibrotic feedback amplification and stiffness-driven

myofibroblast differentiation in lung fibroblasts [42]. Within that context, the preliminary IPF data in Figure 8 and Table 5 are meaningful because they begin to address whether disease-relevant differences in collagen, elastin, and sGAG composition can be retained after decellularization. Because only one male and one female IPF donor were analyzed, these data cannot support definitive conclusions about diseased donor trends; however, they do reinforce the importance of developing disease-representative dECM platforms, since studying lung cells on a matrix that does not appropriately reflect the biochemical and mechanical abnormalities of IPF may fail to reproduce the cues that actually drive disease-associated cell behavior. Expanding diseased-donor analysis in future work will therefore be important for building platforms that more faithfully model IPF ECM composition, matrix stiffness, and the downstream mechanotransductive pathways involved in fibrosis.

This study has several limitations that should be considered when interpreting the findings. First, the healthy human cohort was relatively small, particularly for female donors with n = 3 as compared to n = 5 for males, and the IPF dataset was limited to one male and one female donor, so the diseased-tissue observations should be interpreted as exploratory. Second, the present work focused primarily on biochemical characterization and did not yet include direct mechanical testing, which is important because prior work has shown that normal and fibrotic human lung matrices can differ not only in ECM composition but also in stiffness, and that these mechanical differences can directly influence fibroblast phenotype [40]. This is especially relevant given that human lung dECM hydrogels can reproduce native-like stiffness and viscoelasticity, meaning that future studies will need mechanical characterization to more fully determine how closely these scaffolds replicate the lung microenvironment. Third, although the targeted assays used here provided important information on total protein, collagen, elastin, and sGAG retention, they do not capture the full matrisome, so proteomic or mass spectrometry-based analysis will be necessary in future work to identify additional sex- or disease-associated matrix features that may have been retained or lost during processing. Finally, the viability experiments were performed using NIH 3T3 fibroblasts rather than primary human lung cells, meaning that the present study supports cytocompatibility and early scaffold usability, but does not yet fully define how native human lung cell populations would respond to these matrices in a disease-relevant context.

5. Conclusion and Future Directions

This work establishes decellularized human lung ECM as a promising sex-aware platform for future lung modeling applications. While both SDS-based protocols achieved effective decellularization, the resulting scaffolds were not compositionally equivalent, with 0.1% SDS generally preserving more of the native extracellular matrix than 0.5% SDS. The study further showed that sex-based differences in ECM composition are present, but are often selective and method-dependent, emphasizing that both processing conditions and sex as a biological variable influence the final biochemical identity of the scaffold. Because the resulting dECM supported cell viability and early scaffold integration, these findings extend beyond biochemical characterization alone and support the use of human lung dECM as a biologically relevant material for disease modeling, hydrogel development, and mechanobiology studies. More broadly, this work highlights the importance of building lung models that better preserve native biochemical and microenvironmental complexity, with the long-term goal of enabling more physiologically relevant investigation of fibrosis, cell–matrix interactions, and downstream mechanotransductive signaling.

A key future direction of this work is to expand this human lung dECM system into a more comprehensive sex-aware and disease-relevant modeling platform. Future studies should include a larger number of healthy and IPF donors, particularly female and diseased samples, to better resolve whether the sex- and disease-associated trends observed here are consistent across a broader cohort. In addition to the targeted biochemical assays used in the present study, future work should incorporate proteomic and mass spectrometry-based analysis to define the retained matrisome in greater detail, as well as mechanical characterization to determine how method-dependent differences in ECM composition translate into differences in stiffness, viscoelasticity, and other cell-relevant material properties. These scaffolds should also be further developed into hydrogels and recellularized systems using primary human lung cells, including fibroblasts and other disease-relevant cell populations, to investigate how male- and female-derived healthy and fibrotic matrices differentially regulate cell behavior, matrix remodeling, and mechanotransductive signaling. Ultimately, extending this work in that direction could enable the development of more physiologically relevant human lung models for studying fibrosis mechanisms and for evaluating how sex- and matrix-specific microenvironments shape downstream cellular responses.

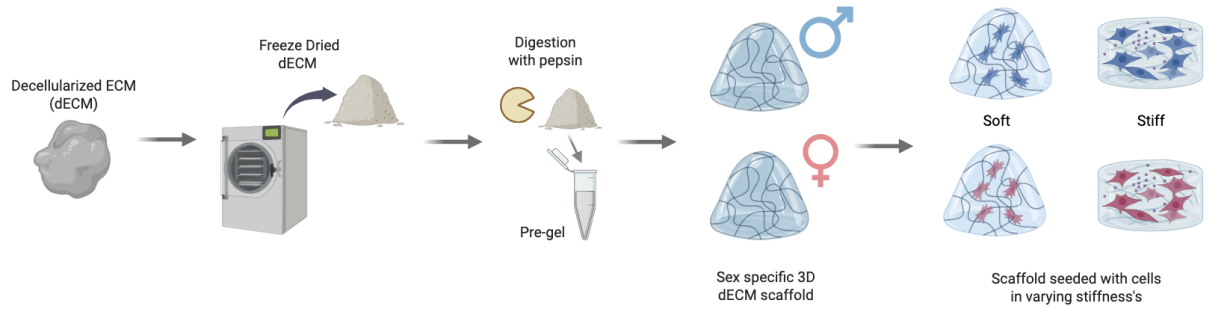


Figure 9. Proposed downstream application of decellularized human lung ECM for sex-specific hydrogel and scaffold generation. Decellularized extracellular matrix (dECM) is freeze-dried, digested with pepsin, and processed into a pre-gel solution for fabrication of sex-specific three-dimensional dECM scaffolds. These materials can then be seeded with cells and used to generate platforms with varying stiffness for future studies of lung cell behavior, matrix remodeling, and mechanobiology.

References

[1] C. Novak, M. N. Ballinger, and S. Ghadiali, "Mechanobiology of Pulmonary Diseases: A Review of Engineering Tools to Understand Lung Mechanotransduction," *J. Biomech. Eng.*, vol. 143, no. 11, p. 110801, Nov. 2021, doi: 10.1115/1.4051118.

[2] A. Naba, "Mechanisms of assembly and remodelling of the extracellular matrix," *Nat. Rev. Mol. Cell Biol.*, vol. 25, no. 11, pp. 865–885, Nov. 2024, doi: 10.1038/s41580-024-00767-3.

[3] J. J. Duggan and R. J. Petrie, "The role of dynamic reciprocity in 3D cell migration: connecting cell and matrix mechanics to migratory plasticity," *Npj Biol. Phys. Mech.*, vol. 2, no. 1, p. 21, Sep. 2025, doi: 10.1038/s44341-025-00027-1.

[4] G. S. Hussey, J. L. Dziki, and S. F. Badylak, "Extracellular matrix-based materials for regenerative medicine," *Nat. Rev. Mater.*, vol. 3, no. 7, pp. 159–173, Jul. 2018, doi: 10.1038/s41578-018-0023-x.

[5] K. Ohata and H. C. Ott, "Human-scale lung regeneration based on decellularized matrix scaffolds as a biologic platform," *Surg. Today*, vol. 50, no. 7, pp. 633–643, Jul. 2020, doi: 10.1007/s00595-020-02000-y.

[6] J. Huang *et al.*, "Extracellular matrix and its therapeutic potential for cancer treatment," *Signal Transduct. Target. Ther.*, vol. 6, no. 1, p. 153, Apr. 2021, doi: 10.1038/s41392-021-00544-0.

[7] O. Courbot and A. Elosegui-Artola, "The role of extracellular matrix viscoelasticity in development and disease," *Npj Biol. Phys. Mech.*, vol. 2, no. 1, p. 10, 2025, doi: 10.1038/s44341-025-00014-6.

[8] A. Saraswathibhatla, D. Indana, and O. Chaudhuri, "Cell–extracellular matrix mechanotransduction in 3D," *Nat. Rev. Mol. Cell Biol.*, vol. 24, no. 7, pp. 495–516, Jul. 2023, doi: 10.1038/s41580-023-00583-1.

[9] S. F. Badylak, D. Taylor, and K. Uygun, "Whole-Organ Tissue Engineering: Decellularization and Recellularization of Three-Dimensional Matrix Scaffolds," *Annu. Rev. Biomed. Eng.*, vol. 13, no. Volume 13, 2011, pp. 27–53, Aug. 2011, doi: 10.1146/annurev-bioeng-071910-124743.

[10] P. M. Crapo, T. W. Gilbert, and S. F. Badylak, "An overview of tissue and whole organ decellularization processes," *Biomaterials*, vol. 32, no. 12, pp. 3233–3243, Apr. 2011, doi: 10.1016/j.biomaterials.2011.01.057.

[11] H. C. Ott *et al.*, "Regeneration and orthotopic transplantation of a bioartificial lung," *Nat. Med.*, vol. 16, no. 8, pp. 927–933, Aug. 2010, doi: 10.1038/nm.2193.

[12] V. Dhandapani, P. Boabekoa, and P. Vermette, "Extracellular matrix from decellularized porcine organs as scaffolds for insulin-secreting cells and pancreatic islets," *Front. Endocrinol.*, vol. 16, Jan. 2026, doi: 10.3389/fendo.2025.1722536.

[13] J. E. Nichols *et al.*, "Production and Assessment of Decellularized Pig and Human Lung Scaffolds," *Tissue Eng. Part A*, vol. 19, no. 17–18, pp. 2045–2062, Sep. 2013, doi: 10.1089/ten.tea.2012.0250.

[14] R. W. Bonvillain *et al.*, "A Nonhuman Primate Model of Lung Regeneration: Detergent-Mediated Decellularization and Initial In Vitro Recellularization with Mesenchymal Stem Cells," *Tissue Eng. Part A*, vol. 18, no. 23–24, pp. 2437–2452, Dec. 2012, doi: 10.1089/ten.tea.2011.0594.

[15] J. D. O'Neill *et al.*, "Decellularization of Human and Porcine Lung Tissues for Pulmonary Tissue Engineering," *Ann. Thorac. Surg.*, vol. 96, no. 3, pp. 1046–1056, Sep. 2013, doi: 10.1016/j.athoracsur.2013.04.022.

[16] A. Gilpin and Y. Yang, "Decellularization Strategies for Regenerative Medicine: From Processing Techniques to Applications," *BioMed Res. Int.*, vol. 2017, p. 9831534, 2017, doi: 10.1155/2017/9831534.

[17] U. Mendibil, R. Ruiz-Hernandez, S. Retegi-Carrion, N. Garcia-Urquia, B. Olalde-Graells, and A. Abarrategi, "Tissue-Specific Decellularization Methods: Rationale and Strategies to Achieve Regenerative Compounds," *Int. J. Mol. Sci.*, vol. 21, no. 15, p. 5447, Jul. 2020, doi: 10.3390/ijms21155447.

[18] P. Tondo *et al.*, "Sex and gender differences during the lung lifespan: unveiling a pivotal impact," *Eur. Respir. Rev.*, vol. 34, no. 175, Feb. 2025, doi: 10.1183/16000617.0121-2024.

[19] P. Silveyra, M. Babayev, and C. D. Ekpruke, "Sex, hormones, and lung health," *Physiol. Rev.*, vol. 106, no. 1, pp. 53–86, Jan. 2026, doi: 10.1152/physrev.00026.2024.

[20] K. Lingappan *et al.*, "Addressing Sex as a Biological Variable in Preclinical Models of Lung Disease: An Official American Thoracic Society Research Statement," *Am. J. Respir. Crit. Care Med.*, vol. 211, no. 8, pp. 1346–1368, doi: 10.1164/rccm.202506-1361ST.

[21] L. R. Simon, A. J. Scott, L. F. Rios, J. Zembles, and K. S. Masters, "Cellular-scale sex differences in extracellular matrix remodeling by valvular interstitial cells," *Heart Vessels*, vol. 38, no. 1, pp. 122–130, Jan. 2023, doi: 10.1007/s00380-022-02164-2.

[22] D. C. Sarver, Y. A. Kharaz, K. B. Sugg, J. P. Gumucio, E. Comerford, and C. L. Mendias, "Sex differences in tendon structure and function," *J. Orthop. Res. Off. Publ. Orthop. Res. Soc.*, vol. 35, no. 10, pp. 2117–2126, Oct. 2017, doi: 10.1002/jor.23516.

[23] L. Matilla *et al.*, “Sex-Differences in Aortic Stenosis: Mechanistic Insights and Clinical Implications,” *Front. Cardiovasc. Med.*, vol. 9, Feb. 2022, doi: 10.3389/fcvm.2022.818371.
[24] L. Sesé *et al.*, “Gender Differences in Idiopathic Pulmonary Fibrosis: Are Men and Women Equal?,” *Front. Med.*, vol. 8, p. 713698, Aug. 2021, doi: 10.3389/fmed.2021.713698.
[25] S. P. McGee, H. Zhang, W. Karmaus, and T. Sabo-Attwood, “Influence of sex and disease severity on gene expression profiles in individuals with idiopathic pulmonary fibrosis,” *Int. J. Mol. Epidemiol. Genet.*, vol. 5, no. 2, pp. 71–86, 2014.
[26] C. Philips, L. Terrie, E. Muylle, and L. Thorrez, “Determination of DNA content as quality control in decellularized tissues: challenges and pitfalls,” *Regen. Biomater.*, vol. 11, p. rbae123, Oct. 2024, doi: 10.1093/rb/rbae123.
[27] T. W. Gilbert, J. M. Freund, and S. F. Badylak, “Quantification of DNA in Biologic Scaffold Materials,” *J. Surg. Res.*, vol. 152, no. 1, pp. 135–139, Mar. 2009, doi: 10.1016/j.jss.2008.02.013.
[28] D. E. Wagner *et al.*, “Comparative decellularization and recellularization of normal versus emphysematous human lungs,” *Biomaterials*, vol. 35, no. 10, pp. 3281–3297, Mar. 2014, doi: 10.1016/j.biomaterials.2013.12.103.
[29] D. M. Faulk *et al.*, “The Effect of Detergents on the Basement Membrane Complex of a Biologic Scaffold Material,” *Acta Biomater.*, vol. 10, no. 1, p. 10.1016/j.actbio.2013.09.006, Jan. 2014, doi: 10.1016/j.actbio.2013.09.006.
[30] F. E. Uhl *et al.*, “Functional role of glycosaminoglycans in decellularized lung extracellular matrix,” *Acta Biomater.*, vol. 102, pp. 231–246, Jan. 2020, doi: 10.1016/j.actbio.2019.11.029.
[31] T. Zaman, T. Moua, E. Vittinghoff, J. H. Ryu, H. R. Collard, and J. S. Lee, “Differences in Clinical Characteristics and Outcomes Between Men and Women With Idiopathic Pulmonary Fibrosis,” *Chest*, vol. 158, no. 1, pp. 245–251, Jul. 2020, doi: 10.1016/j.chest.2020.02.009.
[32] “Biomechanics of the lung parenchyma: critical roles of collagen and mechanical forces | Journal of Applied Physiology | American Physiological Society.” Accessed: Apr. 16, 2026. [Online]. Available: https://journals.physiology.org/doi/full/10.1152/japplphysiol.01087.2004
[33] H. J. Vindin, B. G. Oliver, and A. S. Weiss, “Elastin in healthy and diseased lung,” *Curr. Opin. Biotechnol.*, vol. 74, pp. 15–20, Apr. 2022, doi: 10.1016/j.copbio.2021.10.025.
[34] C. Brasselet *et al.*, “Collagen and elastin cross-linking: a mechanism of constrictive remodeling after arterial injury,” *Am. J. Physiol. Heart Circ. Physiol.*, vol. 289, no. 5, pp. H2228-2233, Nov. 2005, doi: 10.1152/ajpheart.00410.2005.
[35] R. Xu, Y. Du, X. Li, X. Mao, L. Zheng, and M. Zhao, “Differences between soluble and insoluble undenatured type II collagen in improving osteoarthritis in rats and their potential mechanisms,” *Food Funct.*, vol. 14, no. 22, pp. 10240–10251, Nov. 2023, doi: 10.1039/D3FO02954A.
[36] I. Mižíková *et al.*, “Collagen and elastin cross-linking is altered during aberrant late lung development associated with hyperoxia,” *Am. J. Physiol. Lung Cell. Mol. Physiol.*, vol. 308, no. 11, pp. L1145-1158, Jun. 2015, doi: 10.1152/ajplung.00039.2015.
[37] R. H. J. de Hilster *et al.*, “Human lung extracellular matrix hydrogels resemble the stiffness and viscoelasticity of native lung tissue,” *Am. J. Physiol.-Lung Cell. Mol. Physiol.*, vol. 318, no. 4, pp. L698–L704, Apr. 2020, doi: 10.1152/ajplung.00451.2019.
[38] M. Dabaghi *et al.*, “A Robust Protocol for Decellularized Human Lung Bioink Generation Amenable to 2D and 3D Lung Cell Culture,” *Cells*, vol. 10, no. 6, p. 1538, Jun. 2021, doi: 10.3390/cells10061538.
[39] T. Guo, C. He, A. Venado, and Y. Zhou, “Extracellular Matrix Stiffness in Lung Health and Disease,” *Compr. Physiol.*, vol. 12, no. 3, pp. 3523–3558, Jun. 2022, doi: 10.1002/cphy.c210032.
[40] A. J. Booth *et al.*, “Acellular normal and fibrotic human lung matrices as a culture system for in vitro investigation,” *Am. J. Respir. Crit. Care Med.*, vol. 186, no. 9, pp. 866–876, Nov. 2012, doi: 10.1164/rccm.201204-0754OC.
[41] Q. Mei, Z. Liu, H. Zuo, Z. Yang, and J. Qu, “Idiopathic Pulmonary Fibrosis: An Update on Pathogenesis,” *Front. Pharmacol.*, vol. 12, Jan. 2022, doi: 10.3389/fphar.2021.797292.
[42] I. Ganzleben and B. D. Medoff, “Mechanobiology and the extracellular matrix in pulmonary fibrosis,” *iScience*, vol. 28, no. 12, p. 113993, Nov. 2025, doi: 10.1016/j.isci.2025.113993.

Supplemental

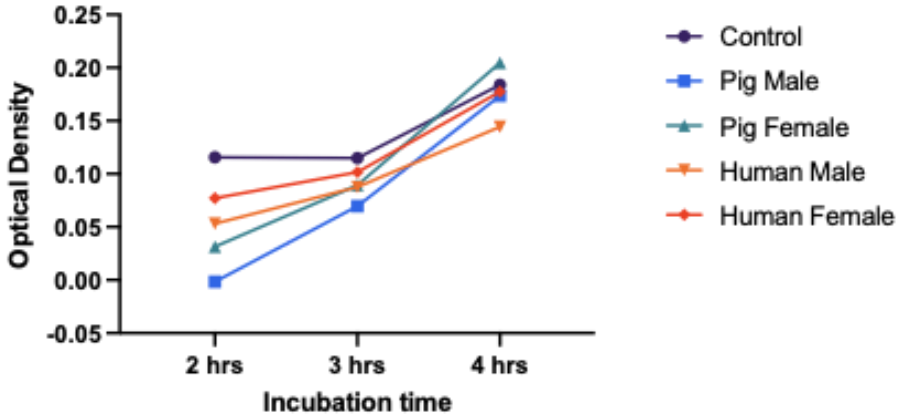


Figure S1. Optimization of the Alamar Blue assay for 3T3 cells seeded in a 48 well plate at a density of 30,000 cells per well. Cells were seeded on day 0. On day 1, Alamar Blue readings were recorded after 2, 3, and 4 hours of incubation. As the highest signal was observed at 4 hours, readings on days 2 and 3 were subsequently measured after 4 hours of incubation.